Photo Processes on Self-Associated Cationic Porphyrins and Plastocyanin Complexes 1. Ligation of Plastocyanin Tyrosine 83 onto Metalloporphyrins and Electron-Transfer Fluorescence Quenching

Hewa M. Anula,[†] Eugene Myshkin,[‡] Anton Guliaev,[||] Charles Luman,[†] Evgeny O. Danilov,[†] Felix N. Castellano,[†] George S. Bullerjahn,*[,‡] and Michael A. J. Rodgers*[,†]

The Center for Photochemical Sciences and Departments of Chemistry and Biological Sciences, Bowling Green State University, Bowling Green, Ohio 43403, and Life Sciences Division, Lawrence Berkeley National Laboratory, Berkeley, California 94720

Received: August 21, 2005; In Final Form: December 3, 2005

The spectroscopic properties of the self-associated complexes formed between the anionic surface docking site of spinach plastocyanin and the cationic metalloporphyrins, in which the tyrosine 83 (Y83) moiety is placed just below the docking site, tetrakis(*N*-methyl-4-pyridyl)porphyrin (Pd(II)TMPyP^{4+} and Zn(II)TMPyP^{4+}), have been studied and reported herein. The fluorescence quenching phenomenon of the self-assembled complex of Zn(II)TMPyP^{4+}/plastocyanin has also been discovered. The observed red-shifting of the Soret and Q-bands of the UV−visible spectra, ca. 9 nm for Pd(II)TMPyP^{4+}/plastocyanin and ca. 6 nm for the Zn(II)TMPyP^{4+}/plastocyanin complexes, was explained in terms of exciton theory coupled with the Gouterman model. Thus, the hydroxyphenyl terminus of the Y83 residue of the self-associated plastocyanin/cationic porphyrin complexes was implicated in the charge-transfer ligation with the central metal atoms of these metalloporphyrins. Moreover, ground-state spectrometric-binding studies between Pd(II)TMPyP^{4+} and the Y83 mutant plastocyanin (Y83F-PC) system proved that Y83 moiety of plastocyanin played a critical role in the formation of such ion-pair complexes. Difference absorption spectra and the Job's plots showed that the electrostatic attractions between the cationic porphyrins and the anionic patch of plastocyanin, bearing the nearby Y83 residue, led to the *predominant formation of a self-associated 1:1 complex* in the ground-state with significantly high binding constants ($K = (8.0 \pm 1.1) \times 10^5$ M^{-1} and $(2.7 \pm 0.8) \times 10^6$ M^{-1} for Pd(II)TMPyP^{4+} and zinc variant, respectively) in low ionic strength buffer, 1 mM KCl and 1 mM phosphate buffer (pH 7.4). Molecular modeling calculations supported the formation of a 1:1 self-associated complex between the porphyrin and plastocyanin with an average distance of ca. 9 Å between the centers of mass of the porphyrin and Y83 positioned just behind the anionic surface docking site on the protein surface. The photoexcited singlet state of Zn(II)-TMPyP^{4+} was quenched by the Y83 residue of the self-associated plastocyanin in a static mechanism as evidenced by steady-state and time-resolved fluorescence experiments. Even when all the porphyrin was complexed (more than 97%), significant residual fluorescence from the complex was observed such that the amplitude of quenching of the singlet state of uncomplexed species was enormously obscured.

Introduction

Photosynthesis is critical to life on earth. Photochemists and photobiologists have focused research on this area for over a century, and emission of light from chlorophyll was first studied in 1834.[1] Intense investigation of the photoproperties of biomimetic model systems for these photosynthetic reaction centers has been inspired by the nature and properties of the "special pair" in these systems. In such biomimetic model systems, the molecules were covalently linked through oligomeric chains[2,3] or spacers,[4] linked by chelating a common metal ion,[5−7] have been self-assembled via axial ligands by formation of cofacial multistacks,[8] or covalently bound to a donor/acceptor residue at specific sites on the surface of the protein.[9−12] Another way of making a cofacial complex between two reaction partners has been to use ion-pair coulombic interactions between oppositely charged components.[13] The formation and photoinduced electron transfer (ET) in electrostatically stabilized self-associated complexes between oppositely charged molecules with biomolecules have been reported.[14−18] The stoichiometry of formation and binding constants of some such complexes have also been documented.[17,19]

Moreover, for a system in which static (associational) and dynamic quenching are present (fluorescence from the complex is assumed to be zero), the emission intensity is given by[20,21]

$$(I_o/I) - 1 = (K_{sv} + \beta K_{eq})[Q] + \beta K_{sv} K_{eq}[Q]^2 \qquad (1)$$

where $\beta = 1$ if the solutions are optically dilute and if the solutions are totally absorbing, I_o and I are the fluorescence intensity in the absence and in the presence of quencher, K_{sv} is the Stern−Volmer constant, K_{eq} is the association constant (binding constant), and Q is the concentration of the quencher. If only associational (static) quenching is present (i.e., $K_{sv} = 0$), *apparently* normal-intensity Stern−Volmer data result. If neither K_{eq} or K_{sv} is zero, nonlinear, upward-curved Stern−

* Corresponding authors: (G.S.B.) E-mail: bullerj@bgnet.bgsu.edu. Phone:419-372-8527.Fax: 419-372-2024.(M.A.J.R.)E-mail: rodgers@bgnet.bgsu.edu. Phone: 419-372-7607. Fax 419-372-9300.

[†] Center for Photochemical Sciences and Department of Chemistry.

[‡] Center for Photochemical Sciences and Department of Biological Sciences.

[||] Lawrence Berkeley Laboratory.

10.1021/jp054712t CCC: $33.50
Published on Web 01/31/2006

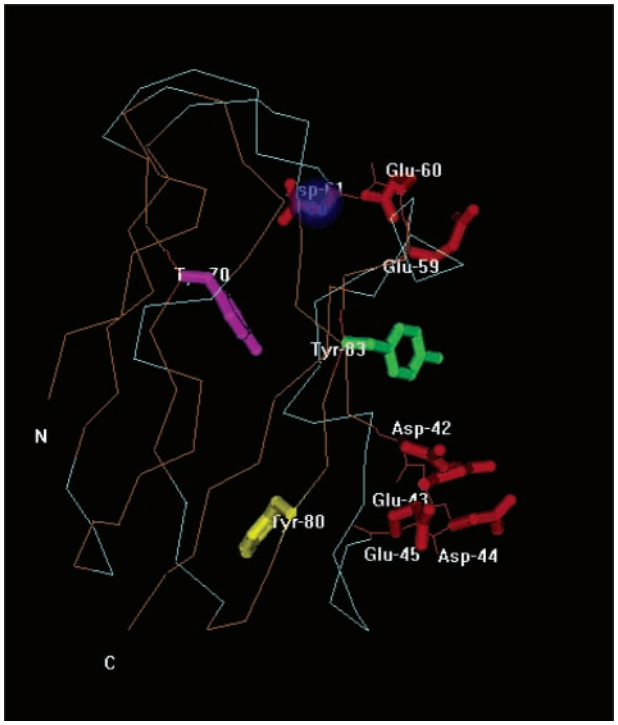

Figure 1. A wire frame model of spinach plastocyanin with the amino acids relevant to this work shown as tube drawings.

Volmer plots will be obtained.[21] Besides, the deviations from linearity of Stern−Volmer plots at higher concentrations of quencher indicate the existence of two populations of fluorophores. The formation of nonfluorescent ground-state complexes results in upward curvatures, and the formation of weakly fluorescent complexes results in downward curvatures.[22] In this paper we report the formation of a strongly fluorescent self-associated ground-state complex of ZnTMPyP^{4+}/plastocyanin (PC) and the generation of a modified Stern−Volmer plot that displays nonlinear upward-curved behavior upon subtraction of residual fluorescence of the complex.

There has been a growing interest in this laboratory in studying the excited-state dynamics (including photoinduced electron-transfer studies) of self-assembled molecular entities via coulombic−electrostatic interactions.[6,7,17,18] Earlier work[18] from this laboratory established evidence for the dynamics in small molecule−protein interactions. Aoudia et al.[18] studied the photo processes in self-assembled complexes of oligopeptides with metalloporphyrins (Pd(II)TMPyP^{4+}, Zn(II)TMPyP^{4+}). Consequently, self-assembled ion pairs between cationic metalloporphyrins (MP) and anionic pentapeptides containing a string of glutamic acid attached to a target reductant, tyrosine or tryptophan terminus (Glu_4Tyr, Glu_4Trp), have been photoexcited in order to study intracomplex ET among the reaction partners with a variable driving force. In the present study we extend this to cofacial porphyrin/PC complexes. Here we used the same coulomb-based electrostatic self-assembly employing positively charged porphyrin units, tetra(*N*-methyl-4-pyridyl)porphyrin chloride salts of palladium(II) and zinc(II) porphyrins (Pd(II)-TMPyP^{4+} and Zn(II)TMPyP^{4+}), and the negatively charged solvent-exposed D and E patch of spinach PC bearing the adjacent solvent-exposed Y83 (see Figure 1). Our hypothesis was that these MPs would form electrostatically stabilized self-associated complexes in aqueous solution with the ,PC which would bring the MP and the hydroxyphenolic ring of the Y83 residue into sufficient proximity that upon photoexcitation of the MP an electron-transfer process would result as had been shown in earlier work in this laboratory with anionic oligopeptides containing tyrosine and cationic porphyrins.[18] The carboxylate residues of the glutamic acid (E, pK_a = 4.3) and aspartic acid (D, pK_a = 3.9) patch of PC are expected to act as an ion-pairing site for the positively charged porphyrins (Figure 1). This paper is concerned largely with spectrophotometric and fluorescence quenching studies (steady-state and time-resolved) of self-assembled cationic porphyrins and PC. In this report we present the novel fluorescence quenching phenomenon for the Zn(II)TMPyP^{4+}/PC complex and the exciting interaction of Y83 ligation onto the metal centers of Pd(II) and Zn(II) of the self-associated cationic porphyrins/PC complexes in which cases the observed red-shifting of the Soret and Q-bands is explained in terms of the Gouterman model coupled with exciton theory.

Experimental Section

Materials. Mesotetrakis(*N*-methyl-4-pyridyl)porphyrin tetrachloride salts of palladium(II) and zinc(II) were used as received from Porphyrin Products. Sucrose, antifoam A, Sepharose 4B, Bio-Rad AG1 X8 resin, and Trizma base were obtained from Sigma in the highest available purity grade. Potassium chloride (99%, Sigma), ammonium sulfate (99%, Sigma), potassium ferricyanide (99%, Sigma), acetone (spectroscopic grade, Sigma), and monobasic and dibasic potassium phosphate (99%, Sigma) were used as received. Tube-O-Dialysers (MW cutoff 8000, 3.0 mL) were obtained from Genotechnology Inc., Amicon ultrafiltration units (YM10 membrane) were purchased from Millipore Corporation (centriprep centrifugal filter devices).

Protein Purification in Spinach Chloroplasts. The preparation of PC was based on the methods of Ellefson et al.[23] and Ashton and Anderson.[24] In the present investigation the extraction and purification of PC were carried out as described previously by Krogmann and co-workers,[25] which combines the two procedures mentioned above.

The purity of the protein was determined by a single band (10 kDa) in the sodium dodecyl sulfate−polyacrylamide gel electrophoresis (SDS−PAGE) analysis. The protein concentration was determined by using the extinction coefficient of tyrosine (1.4×10^3 M^{-1} cm^{-1})[26] since no tryptophan residues are present in spinach PC, and a value of 620 μM (sample 1) was obtained for the concentration of protein. A second preparation of the same protein yielded a concentration of 690 μM (sample 2). The estimation of concentration by this method was the most appropriate technique for all the experiments described in this paper, even though this method does not take into account the environmental influence on the extinction coefficients of tyrosine.

Expression of Spinach PC in *Escherichia coli*. Spinach PC and the Y83F mutant PC were expressed in *E. coli* as inclusion bodies and reconstituted with copper to yield a preparation having identical UV−visible (UV−vis) and circular dichoism (CD) spectroscopic properties as those of the native protein purified from leaves. Our expression system is essentially the same as that described earlier for production of *Prochlorothrix hollandica* PC.[27,28] Specifically, the spinach PC coding sequence for mature PC was obtained by polymerase chain reaction (PCR) of spinach genomic DNA. PCR was performed over 30 cycles with a temperature regime of 1 min at 94 °C → 2 min at 45 °C → 3 min at 72 °C with the following primers (restriction sites are underlined and the start and termination codons are in bold):

5' primer: 5'-GGCGGC<u>GCTAGC</u>**ATG**GTTGAGGTGTTGCTCGGAGGGGG-3'

3' primer: 5'-GGCGGC<u>GGATCC</u>**TTA**GTTGACAGTTACTTTTCCCACC-3'

Such primers yielded a 326 bp product having 5′ *Nhe* I and 3′ *Bam* HI restriction sites that were cloned in-frame into (*Nhe* I/*Bam* HI)-cleaved pVAPC10, a T7 RNA polymerase-dependent expression plasmid constructed exclusively for PC expression.[27,28] Induction of the PC gene, purification of inclusion bodies, and reconstitution of PC holoprotein were as described previously[27,28] except that the pVAPC10 *E. coli* host was Novagen Rosetta, a modified BL21 (DE3) strain better capable of accommodating the spinach PC gene codon bases specifying arginine, glycine, proline, and alanine.

Construction of PC Mutant Y83F. A mutagenic DNA oligonucleotide primer (5′-GGAACTTACAAGTTCTTTTGCTCACCCCACCAGG-3′) covering codons 78−89 of the mature protein was synthesized; this sequence replaces a TAC codon with TTT specifying phenylalanine (F) at position 83 (underlined above). The primer was used for PCR of pVAPC10 plasmid DNA containing the wild-type spinach PC gene. The resulting mutagenized gene was verified by DNA sequencing and transformed into the *E. coli* BL21(DE3) Rosetta strain. Expression and reconstitution of the Y83F mutant PC followed standard procedures.[27,28]

All solutions were prepared with distilled water purified by a Barnsted E NANOpure II water purification system. The original potassium phosphate buffer (pH 7.4, 100 mM ionic strength) was prepared with monobasic and dibasic potassium phosphate (99%, Sigma). Ionic strengths were adjusted by adding KCl.

Molecular-Dynamics (MD) Calculation. The three-dimensional coordinates of spinach PC were obtained from the Brookhaven Protein Data Bank (ID: 1AG6). All molecular modeling was performed using the Amber 7.0 software package. To model interactions between the protein and porphyrin MD simulations made with a Cornel force field were utilized to obtain final conformations for the PC/porphyrin complex. The set of force field parameters and geometry optimized coordinates for the porphyrin molecule was previously developed with ab initio quantum mechanical calculations using a Spartan 5.0 suite (Wavefunction, Inc., Irvine, CA). The PC molecule was initially subjected to a series of the free energy minimization runs. Twelve starting conformations were generated by placing the porphyrin molecule with 15° intervals along a 180° arc above the protein anionic patch. In each case the plane defining the core of the porphyrin molecule was parallel to the surface of the PC, and the porphyrin was placed approximately 30−35 Å away from the protein surface. Each starting conformation (12 total) was subjected to the 50 ps MD to optimize electrostatic interactions between the anionic aspartic and glutamic acid residues, D42, E43, D44, E45, D51, E59, E60, and D61 and the cationic *N*-methyl pyridyl groups of cationic porphyrins. A distance-dependent dielectric constant was used to simulate the presence of the high dielectric solvent. All simulations were performed using a 2 fs time step, and all hydrogens were constrained using the SHAKE algorithm. The distance and angle between chromophores of the two molecules were calculated during the last 30 ps of the MD runs. The data for all 12 conformations are summarized in Table 1. The complex visualization was performed using the Insight II (MSI, Biosym).

UV−Vis Spectrometric Studies. Spectrophotometric measurements were performed on a Varian Cary 50 UV−vis spectrophotometer (single beam) with a resolution of ±1 nm. Difference spectra, Jobs's[29] plots, and spectrometric titrations were obtained following the method of Lipskier and Tran-Thi[30] using a 10 mm optical path length quartz cuvette at 25 °C. In each measurement, the sample was referenced to the solvent (1 mM phosphate buffer at pH 7.4) in a matched cuvette.

TABLE 1: InterChromophore Parameters and Total Energies of 12 Runs

run #	IC distance (Å)	IC angle (deg)	energy (cal/mol)
1	7.02 ± 0.26	65.09 ± 5.02	−1155.3
2	10.53 ± 0.21	57.21 ± 5.75	−1108.7
3	10.44 ± 0.29	54.21 ± 6.27	−1094.0
4	5.40 ± 0.30	51.11 ± 4.42	−1165.4
5	5.40 ± 0.25	48.82 ± 3.84	−1152.6
6	10.53 ± 0.21	57.21 ± 5.75	−1108.7
7	10.29 ± 0.90	56.89 ± 8.08	−1087.2
8	12.33 ± 0.28	47.85 ± 11.64	−1086.5
9	12.185 ± 0.38	110 ± 4.35	−1082.2
10	8.85 ± 0.24	51. 66 ± 17.55	−1078.4
11	8.78 ± 0.462	54.38 ± 7.56	−1102.2
12	5.44 ± 0.13	35.81 ± 0.13	−1122.7
Average	**8.93 ± 2.56**	**58.10 ± 18.74**	**−1112.0 ± 30.47**

All spectrophotometric titrations were performed in a 1 cm quartz cuvette. In all cases the concentration of the porphyrins was 5 μM in 1 mM phosphate buffer (pH 7.4) and 1 mM KCl. In the case of Pd(II)TMPyP^{4+} the PC sample of concentration 620 μM (sample 1) was used in the titration at first. To reproduce this set of titrations for Pd(II)TMPyP^{4+} and for the titration with Zn(II)TMPyP^{4+}, the protein sample of the second preparation (sample 2) of concentration 690 μM was used. The pH was measured with a calibrated Corning ion analyzer (model 250).

Steady-State Fluorescence Measurements. Fluorescence spectra were obtained using a single photon counting spectrofluorimeter from Edinburgh Analytical Instruments (FL/FS 900). The temperature of the sample was maintained at 25 ± 1 °C for all measurements by means of a Neslab RTE-111 circulating bath. Excitation at 550 nm was achieved with a 450 W Xe lamp optically coupled to a monochromator (±2 nm), and emission was collected at 90° and passed through a second monochromator (±2 nm). A Peltier-cooled (−30 °C) red-sensitive photomultiplier tube (PMT), R955, was used to register the emission. The excitation wavelength at 550 nm was chosen so that the absorbance of each sample was 0.05/cm at the excitation wavelength and so that the fraction of light absorbed by the Zn(II)TMPyP^{4+}/PC complex was predominant over that absorbed by Zn(II)TMPyP^{4+} (the absorbance ratio of the complex to uncomplexed at 550 nm, A_{ZnPpc}/A_{ZnP}, varied from 4.2 to 42 in the concentration range of PC investigated: 6.6−42.3 μM). The optically matched samples were used so that the number of absorbed photons was kept constant for all the solutions containing Zn(II)TMPyP^{4+}/PC mixtures.

Time-Correlated Single Photon Counting Measurements. Fluorescence lifetimes were obtained by using the same instrument described in the preceding paragraph. The sample cuvette was maintained at 25 °C. Excitation was accomplished with a pulsed light source (PLS-8-2-079) controlled by a PicoQuant driving unit (PDL 800-B pulsed diode laser). The light source provided a 2.5 MHz train of pulses (700 ps fwhm) at 455 nm. The time resolution of the instrument, 700 ps, was determined from the fwhm of the instrument response function (IRF) and of the time profile of the excitation pulse. At this wavelength of excitation, 455 nm, the predominant absorbing species was the Zn(II)TMPyP^{4+}/PC complex as evidenced by the difference absorption spectra (the absorbance ratio of the complex to uncomplexed at 455 nm, A_{ZnPpc}/A_{ZnP} varied from 2.6 to 50 in the concentration range of PC used, 10.5−39.0 μM). The time-resolved single photon counting procedure using

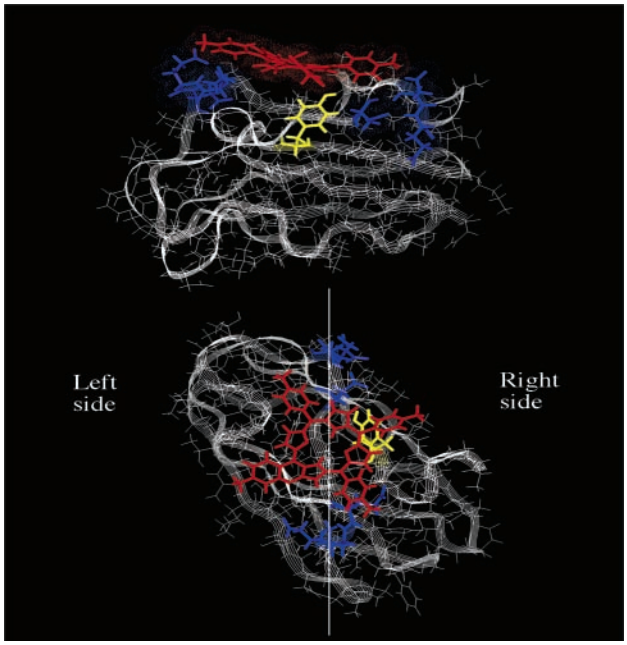

Figure 2. The side (upper picture) and top views (bottom picture) of the final conformation (complex 1) of the plastocyanin/porphyrin complex. The porphyrin is in red, Tyr 83 is in yellow, the anionic patch is in blue, and the protein is in gray. The van der Waals radii are shown for the porphyrin and amino acids forming the anionic patch on the side view. Left and right sides discussed in the text are indicated on the top view.

this system has been described.[31] Samples were optically matched at 455 nm so that the results were on a per photon absorbed basis. The data were analyzed by deconvolution of the emission decay profile with the IRF using Edinburgh Instruments software.

Results

Molecular-Dynamic Calculation. Figure 2 shows side (upper picture) and top views (bottom picture) of the final conformation (complex 1) for the PC/porphyrin complex modeled by the MD procedure outlined above. The 12 different starting conformations each generated a distribution of Tyr 83-to-PdTMPyP^{4+} interchromophore distances and interchromophore angles (Table 1). The 12 determinations yielded averages of 8.93 $\pm$ 2.56 Å and 58.10 $\pm$ 18.74° for the two parameters. As suggested, the interaction between the porphyrin and PC molecules should be strongly influenced by the coulombic forces. Additionally, the simulation during the last 30 ps of the MD procedure revealed that the carboxylate end termini of the D and E residues of the 2 anionic surface docking site of PC (Figure 1) form an anionic template with which the four quaternary N atoms of the pyridyl mesosubstituents of porphyrin self-associate to form a 1:1 docking complex.

Ground-State Difference Spectra. The interaction between the cationic porphyrins and PC was studied in aqueous solutions at physiological pH (7.4) with low ionic strength buffer (1 mM KCl) at 25 °C. The difference spectra (Figure 3) of PC and porphyrin mixtures were obtained by subtraction of a few of the spectra obtained after mixing (Pd(II)TMPyP^{4+}/PC complex) from that obtained before mixing (pure porphyrin). Experiments completed by using a tandem-mixing cell yielded the same results. Scrutiny of the spectra showed the predominant absorption by the complex and the band intensity in the Soret region increased with the increase of PC concentration and subsequently leveled off at the most predominant complexation. Also

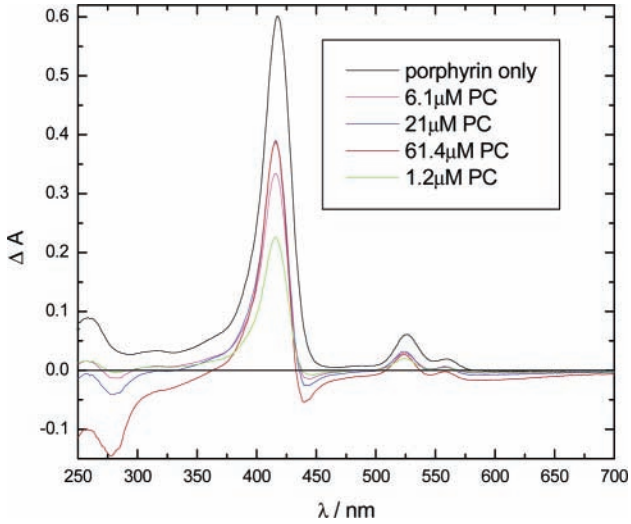

Figure 3. Difference spectra obtained by subtraction of a few of the spectra obtained after mixing (Pd(II)TMPyP^{4+}/plastocyanin complex) from that obtained before mixing (pure porphyrin). The concentration of Pd(II)TMPyP^{4+} is 5 μM (25 °C, pH = 7.4, 1 mM phosphate buffer, and 1 mM KCl). The concentrations of plastocyanin indicated above were 1.2, 6.1, 21.0, and 61.4 μM. The porphyrin only spectrum is in absorbance, A, units.

the negative peak in the range 425−450 nm is a clear indication that both the Pd(II)TMPyP^{4+} and the complex absorb in the same region and that the extinction coefficient of the complex in this region is higher than that of Pd(II)TMPyP^{4+}. The observed spectral changes are reminiscent of those described in the literature,[32] in which monomeric reactants are in equilibrium with a complex (see below) such that the spectra of one of the monomers and that of the complex overlap but the other monomer does not absorb. A series of experiments involving Zn(II)TMPyP^{4+} and PC showed similar spectral behavior.

Spectrophotometric Titrations. Figure 4 shows the spectral change of the Soret band of Pd(II)TMPyP^{4+} (5 μM, 1 mM phosphate buffer, pH = 7.4, 1 mM KCl) upon titration with aliquots of PC (0.5−54 μM). As the PC concentration increased, the intensity of the Soret band maximum decreased with a slight red-shift of the band maxima, ca. 9 nm (Figure 4). At the higher concentrations of PC, an isosbestic region was also seen centered at ca. 430 nm that is indicative of complex formation. However, the isosbestic point for a clean formation of the 1:1 complex (Job's plot) was slightly smeared because of the detection of scattered light from the generation of a trace of turbidity typical of protein solutions.[26] The overlapping absorption spectra of the complexes and of the uncomplexed Pd(II)TMPyP^{4+} in the entire Soret region as shown in Figure 3 also accounts in part for the detection of a less clean isosbestic point in this case. The inset of Figure 4 shows similar spectral behavior for the Q-band region (ca. 6 nm red-shift). In addition to the similar effects seen in the Soret region, a new absorption band is seen at the red side of the Q-bands that increases as the concentration of PC increases. This arises from the ligand-to-metal charge transfer (LMCT) [S(Cys) $\rightarrow$ Cu^{2+}] absorption of the Cu(II) center.[9] However at a high protein concentration (above ca. 35 μM) the absorbance at the Soret band started to increase. This result is consistent with the fact that both the complex and the unbound porphyrin absorb in the same region (Soret). Thus, the evidence for ion association is clearly demonstrated by the effect on the ground-state absorption of Pd(II)TMPyP^{4+} of increasing the PC concentration. Positively charged molecules such as [Co(phen)$_3$]$^{3+}$ have been shown to interact with the acidic patch of PC centered on Y83 [33] in addition to the well-

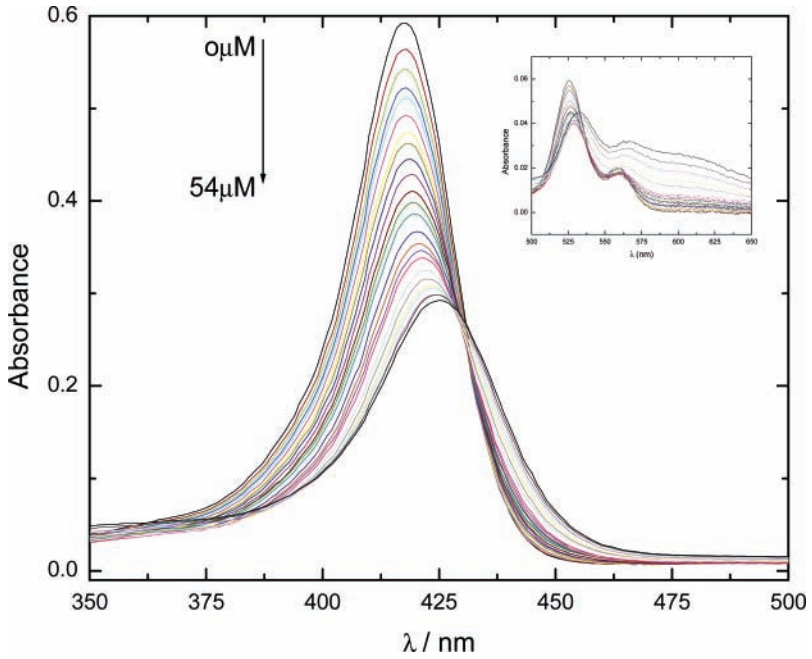

Figure 4. Spectrophotometric titration of Pd(II)TMPyP^{4+} (5 μM in 1 mM phosphate buffer, pH = 7.4 and 1 mM KCl) with addition of plastocyanin at 25 °C. The concentration of plastocyanin added varied from 0 to 54 μM. The inset shows the spectral changes in the Q-band region.

known interactions of the acidic patch with its reaction partners, cytochromes *c* and *f* and photosystem I.[34,35]

A spectrophotometric titration of Zn(II)TMPyP^{4+} (5 μM, 1 mM phosphate buffer, pH = 7.4, 1 mM KCl) with PC yielded very similar results to those obtained in the Pd(II)TMPyP^{4+} case (data not shown). As the PC concentration increased (0.3−48.4 μM), the intensity of the Soret band maximum decreased with a slight red-shift of the band maximum (6 nm). A smeared isosbestic region centered at ca. 448 nm was also noted in this case as indicative of the detection of scattered light from the generation of a trace of turbidity typical of protein solutions at the instant of excitation.

To investigate the role of tyrosine on the complexation between cationic porphyrins and the anionic patch of PC, a similar spectrophotometric titration was carried out between Pd(II)TMPyP^{4+} and the polyglutamic acid peptide system (average molecular weight of 1125 and average number of glutamic acid of 7) in which the target tyrosine moiety was not present. This oligomer was chosen to mimic the acidic patch (glutamic and aspartic) of the native protein PC. Figure 5 shows the spectral change of Pd(II)TMPyP^{4+} (5 μM, 10 mM phosphate buffer, pH = 7.4, 1 mM KCl) upon titration with a small aliquot of polyglutamic acid in which case the concentration of the oligopeptide varies from 1.0−20 μM in glutamic acid monomer units. As the concentration of the oligopeptide increased, the intensity of the Soret band maxima started to decrease and an isosbestic point was also identified at 436 nm, indicative of complex formation. Similar spectral behavior was observed for the Q-bands.

Job's Plots. The most widespread method to determine the stoichiometry of the mixed complexes is Job's method.[29] The method is an effective and reliable approach to the determination of the stoichiometry of the complexes. This method depends on the fact that the optical density of a mixture of chromophores which do not react with each other is the sum of the absorptions due to each chromophore separately. Evidence of the formation of a complex can be obtained from the departures from additivity as the composition of the solution is continuously varied. A Job's diagram is made by plotting the amplitude of the departure

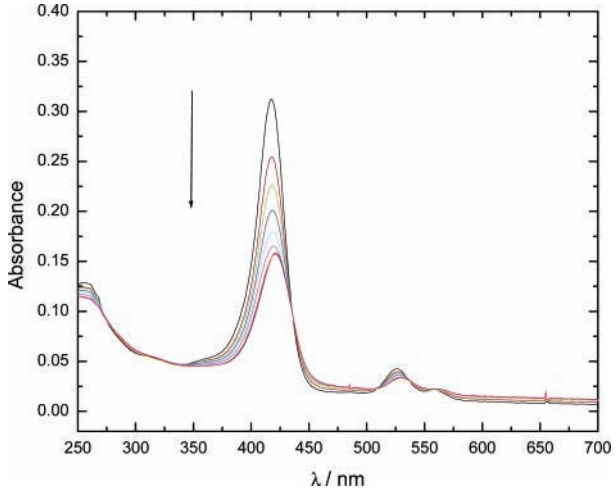

Figure 5. Spectrophotometric titration of Pd(II)TMPyP^{4+} (5 μM in 10 mM phosphate buffer at pH 7.4 and 1 mM KCl) with the addition of 500 μM polyglutamic acid (oligomer with average number of glutamic acid equal to 7) in 10 mM phosphate buffer and 1 mM KCl at 25 °C. The concentration of polyglutamic acid added varied from 0 to 20 μM in glutamic acid monomer unit concentrations.

versus the composition of the mixture. The composition at which the maximum deviation appears can be interpreted as the stoichiometry of the complex. In practice, the absorptions measured at a given wavelength (417 nm for palladium porphyrin) for mixtures with various ratios of porphyrin and PC have been used together with the expression

$$F(x) = \mathrm{d}(x) - (\epsilon_{\mathrm{pd}} - \epsilon_{\mathrm{pc}})x - \epsilon_{\mathrm{pc}}$$

where x is the molar fraction of Pd(II)TMPyP^{4+} or Zn(II)TMPyP^{4+}, ϵ_{pd} and ϵ_{pc} are the molar absorptivities of the Pd(II)TMPyP^{4+}(Zn(II)TMPyP^{4+}) and PC, respectively, and d(x) is the actual absorbance of the solution divided by the total concentration of chromophores. Thus $F(x)$ represents the deviation from the additivity of the absorption of a mixture of x Pd(II)TMPyP^{4+} (Zn(II)TMPyP^{4+}) and (1 − x) M PC in molar absorption units. Job's diagrams are obtained by plotting $F(x)$

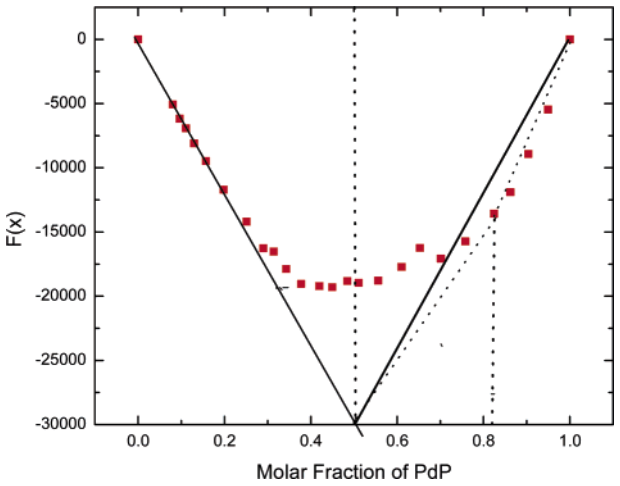

Figure 6. Job's plot for the Pd(II)TMPyP^{4+}/plastocyanin mixture in 1 mM phosphate buffer (pH = 7.4) and 1 mM KCl measured at 417 nm.

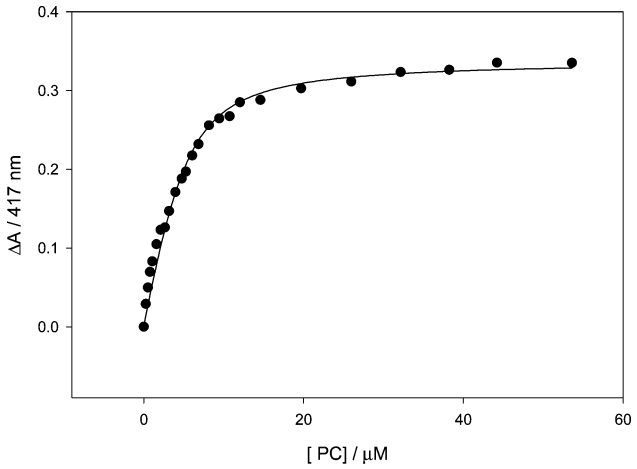

Figure 7. A plot of ΔA (417 nm) versus concentration of plastocyanin for the Pd(II)TMPyP^{4+}/plastocyanin complex to determine the binding constant in 1 mM phosphate buffer (pH = 7.4) and 1 mM KCl.

as x is continuously varied. Figure 6 represents the Job's plot for Pd(II)TMPyP^{4+} (5 μM, 1 mM KCl, 1 mM phosphate buffer, pH = 7.4)/PC mixtures. A similar diagram was generated for the Zn(II)TMPyP^{4+} (5 μM, 1 mM KCl, 1 mM phosphate buffer, pH = 7.4)/PC mixtures. The wavelengths chosen for the Job's diagrams were the center of the Soret band (417 nm) for the Pd(II)TMPyP^{4+}/PC complex and the center of the Soret band (437 nm) for the Zn(II)TMPyP^{4+}/PC system to get the best signal-to-noise ratio. The titration data for both systems resulted in Job's plots with predominant formation of 1:1 stoichiometric complexes.

Binding Constants. Analysis of the Job's plot shown in Figure 6 clearly indicated that the observed difference spectra (Figure 3) arise from the equilibrium-predominant formation of a 1:1 self-association complex between Pd(II)TMPyP^{4+} and the anionic patch of the PC. The MD calculation also clearly supports the formation of this 1:1 stoichiometric docking complex.

$$\text{Pd(II)TMPyP}^{4+} + \text{PC} \rightleftharpoons \text{Pd(II)TMPyP}^{4+}\text{:PC}$$

Additionally, this finding is substantiated by titration curves and is consistent with previous studies in which cytochrome c was reported to be bound to PC in such a way that the cationic lysine patch around the exposed heme edge on the protein abuts an area within the negative patch of PC.[36] Thus, for the complex formation with 1:1 stoichiometry, the change of ΔA (417 nm) as a function of initial concentration of plastocyanin, $[PC]_o$, at constant initial concentration of Pd(II)TMPyP^{4+}, $[PdP]_o$, can be described by eq 2 in which case we considered the fact that both Pd(II)TMPyP^{4+} and the complex absorb at 417 nm.

$$\Delta A = \frac{([PdP]_o + [PC]_o + K^{-1}) - \{([PdP]_o + [PC]_o + K^{-1})^2 - 4[PdP]_o[PC]_o\}^{0.5}}{2/\Delta\epsilon} \quad (2)$$

where K is the binding constant and $\Delta\epsilon$ is the difference of molar absorptivities between Pd(II)TMPyP^{4+} and the complex at 417 nm. The titration data were fitted to the above equation (Figure 7) using a nonlinear regression program. This yielded a binding constant of $(8.0 \pm 1.1) \times 10^5$ M^{-1} in very low ionic strength buffer (1 mM KCl, 1 mM potassium phosphate, pH = 7.4). The extinction coefficient of the complex was extracted from the regression parameters, and a value of $(4.6 \pm 0.6) \times 10^4$ M^{-1} cm^{-1} was obtained for the Pd(II)TMPyP^{4+}/PC complex at 417 nm. Moreover, the excellent nonlinear fit in this case (Figure 7) provided supportive evidence for the formation of a 1:1 docking complex for which the above equation was derived on a mixture of chromophores interacting to form 1:1 stoichiomeric complexes.

A similar analysis of Job's plot and titration data for the Zn(II)TMPyP^{4+}/PC system yielded an extinction coefficient of $\epsilon_{437} = (6.5 \pm 0.4) \times 10^4$ M^{-1} cm^{-1} and a binding constant of $K = (2.7 \pm 0.8) \times 10^6$ M^{-1} (data not shown) in the same solution conditions. In addition, a similar series of titration data for the freebase H_2TMPyP^{4+} and PC complexation yielded a binding constant of 3.5×10^5 M^{-1} in very low ionic strength buffer (1 mM KCl, 1 mM potassium phosphate buffer, pH = 7.4).

Studies with Tyrosine 83 Mutant Plastocyanin (Y83F-PC). *Association of Y83F-PC and PdTMPyP^{4+}.* To test the hypothesis of this project that the electron-transfer processes arise from the Y83 residue located just behind the anionic surface docking site of the native PC, control experiments were conducted on a Y83 mutant plastocyanin (Y83FPC) in which Y83 was substituted by a F. The ground-state spectrum of Y83F-PC in 1 mM phosphate buffer (pH = 7.4) displayed a band centered at 250 nm (data not shown), which is characteristic of F present in PC.[26,37] A intense band centered at 275 nm for the lowest energy singlet electronic transition ($\pi-\pi^*$) of tyrosine[38] was absent in this Y83 mutant (Y83F) PC; instead a broad band in the range 225−300 nm was present, indicative of a correct substitution of F having taken the place of the solvent-exposed Y83 of PC.

Ground-state spectrophotometric titration between Y83F-PC and solutions of Pd(II)TMPyP^{4+} in 1 mM phosphate buffer (pH = 7.4, 1 mM KCl) indicated ion-pairing interactions on the basis of the decrease of the Soret and Q-bands intensity on the addition of mutant PC. The observed intensity changes in the absorption spectra was interpreted by assuming the formation of a 1:1 complex between Pd(II)TMPyP^{4+} and Y83F-PC as observed in the 1:1 stoichiometry for the porphyrin/native PC system. The binding constant for the association of Pd(II)TMPyP^{4+} and Y83F-PC was obtained by a plot of ΔA (417 nm) versus the concentration of Y83F-PC as obtained for the porphyrin/PC systems. A least-squares fitting analysis of the plot yielded a value of $K = 7.0 \times 10^4$ M^{-1} for the binding constant compared to a value of $K = 8.0 \times 10^5$ M^{-1} for the Pd(II)TMPyP^{4+}/native PC self-assembly. Thus, these results along with the spectrometric binding studies on the Pd(II)TMPyP^{4+}, Zn(II)TMPyP^{4+}, and the freebase systems clearly

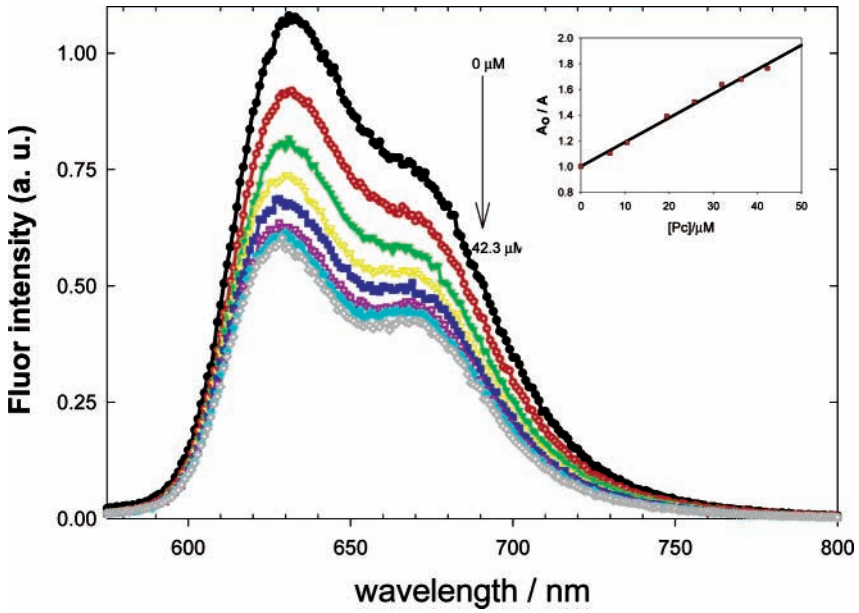

Figure 8. Spectral changes of the fluorescence spectra of Zn(II)TMPyP^{4+}/plastocyanin mixtures in aqueous solution (1 mM KCl, 1 mM phosphate buffer, pH = 7.4) at 25 °C. The indicated spectra corresponds to the 0, 6.6, 10.5, 19.4, 25.7, 31.9, 36.3, and 42.3 μM plastocyanin in the mixtures. Excitation was at 550 nm. Inset: The ratio of normalized integrated area of fluorescence A_o/A as a function of concentration of plastocyanin at 25 °C, pH = 7.4, 1 mM KCl, and 1 mM phosphate buffer (pH = 7.4).

TABLE 2: Calculated % Complexation of Zn(II) Porphyrin for Various Concentrations of Plastocyanin and Observed Percentage of Fluorescence Quenching at Each Concentration

[PC] (μM)	% Zn(II)P complexed	% quenching at 632 nm
0	0	0
6.6	74.1	15
10.5	85.9	24.3
19.5	93.6	31.6
25.7	95.4	36.4
31.9	96.4	41.2
36.3	96.9	43.1
42.3	97.4	44.2

reveal that Y83 plays a critical role on the formation of these self-associated complexes.

Steady-State Fluorescence Measurements. A study of the quenching of fluorescence of Zn(II)TMPyP^{4+} by PC was carried out at pH 7.4 (1 mM phosphate buffer) in low ionic strength buffer (1 mM KCl). The excitation wavelength (550 nm) was chosen so that the absorbance of each sample containing the PC were optically matched to have an optical density of 0.05 cm^{-1} and so that the fraction of light absorbed by the Zn(II)-TMPyP^{4+}/PC complex was predominant over that absorbed by the Zn(II)TMPyP^{4+} as evidenced by the difference absorption spectra (data not shown). Besides, at this wavelength of 550 nm, the absorbance ratio of the complex to uncomplexed Zn-(II)TMPyP^{4+}, A_{ZnPpc}/A_{ZnP}, was varied between 4.2 and 42 in the concentration of plastcyanin of 6.6−42.3 μM used. When PC was present (up to 42.3 μM, 97.4% complex), the fluorescence intensity of Zn(II)TMPyP^{4+} was quenched (Figure 8), and the fraction of quenching started to increase and leveled off to ca. 50% at a high PC concentration (Table 2). The fraction of quenching in each mixture did not correlate with the fraction of Zn(II) porphyrin that was complexed with the protein (Table 2). This result indicates that a significant amount of fluorescence of the complex must appear in the same wavelength region as that of uncomplexed porphyrin. Indeed, the overlapping fluorescence of the complex is clearly evident by the deconvoluted difference fluorescence spectra and the observed excitation spectrum of the Zn(II)TMPyP^{4+}/PC mixture.

Difference Fluorescence Spectra and the Fluorescence of the Complex. The above results show that the fluorescence intensity quenching is about ca. 50% at low ionic strength (1 mM), but the Stern−Volmer plot (inset of Figure 8) is linear despite the efficient ground-state complex formation (Table 2).[21] It was deemed essential to make a correction for the residual fluorescence of the complex by which the anticipated upward-curved nonlinear behavior of Stern−Volmer plot for the bimolecular dynamic quenching was obscured in the presence of ground-state complexation (eq 1).[21] Thus, to find out the residual fluorescence of the complex, a set of difference fluorescence spectra were obtained by subtraction (Table 3.*)* of each of the fluorescence spectra of the mixtures from the fluorescence spectrum of pure Zn(II) porphyrin (inset of Figure 9). Interestingly, these observed difference fluorescence spectra for each PC concentration (% of Zn(II) porphyrin complexed varied from 74.1 to 97.4) predominantly represent the fluorescence spectra of the self-associated complex between PC and Zn(II) porphyrin. Scrutiny of Figures 8 and 9 led to another interesting observation that at the highest concentration of PC (42.3 μM), in which more than 97% of the porphyrin molecules are present in complexed form, the quantum yield of fluorescence of the complex is ca. 50% compared to that of the free compound.

Figure 9 shows the modified Stern−Volmer plot that was obtained by using the ratio of the integrated fluorescence, (A_o/A_{free}) corrected for the residual fluorescence of the complexes shown in Table 3. The results along with the data in Table 3 show that there is efficient quenching at low ionic strength (1 mM) and the Stern−Volmer plot is nonlinear with upward-curvature from which the supportive evidence is revealed for the predominant static fluorescence quenching and for the formation of the pseudo-nonfluorophore ground-state complex in this case as well (eq 1).[21]

This finding was substantiated by the excitation spectrum that was obtained for the (5 μM) Zn(II) porphyrin/PC (42.3 μM) mixture by scanning the excitation wavelength over a 250−600 nm range and monitoring the fluorescence at 632 nm. Figure 10 shows the observed excitation spectrum of (5 μM) Zn(II) porphyrin in the presence of PC (42.3 μM, 97.4% complex) in

TABLE 3: Integrated Area of Difference Fluorescence Spectra and the Fluorescence Data for the Complexes in Each Case and the Calculated Percentage of Quenching for the Modified Stern−Volmer Plot in Each Concentration

[PC] (μM)	% Zn(II)P complexed	[a] $A_{difference}$	[a] $A_{complex}$	[b] A_{free}	% intensity [c] quenching [d]
0	0	0	0	1.6×10^6	0 (1)
6.6	74.1	2.4×10^5	1.8×10^5	1.2×10^6	25 (1.3)
10.5	85.9	4.2×10^5	3.6×10^5	9.4×10^5	41.2 (1.7)
19.5	93.6	5.3×10^5	4.9×10^5	6.2×10^5	61.2 (2.6)
25.7	95.4	6.0×10^5	5.7×10^5	4.7×10^5	70.6 (3.4)
31.9	96.4	6.8×10^5	6.6×10^5	3.1×10^5	80.6 (5.2)
36.3	96.9	7.2×10^5	6.9×10^5	2.3×10^5	85.6 (7.0)
42.3	97.4	7.6×10^5	7.4×10^5	1.5×10^5	90.6 (10.7)

[a] Difference fluorescence spectra were obtained by subtraction of the spectra obtained after mixing (5.0 μM ZnTMPyP^{4+}/plastocyanin complexes for the mixtures in the concentrations 6.6, 10.5, 19.4, 25.7, 31.9, 36.3, and 42.3 μM of plastocyanin) from that obtained before mixing (pure ZnTMPyP^{4+} fluorescence). In each case, the observed fluorescence for porphyrin/protein mixtures was corrected for the fluorescence of the complexes. The integrated area of fluorescence from the complex was obtained by the relationship $A_{complex} = A_{difference\ fluorescence} \times$ % complexation. [b] The integrated area of the fluorescence spectra between 575 and 750 nm was calculated for all porphyrin/protein mixtures and it was indicated as "*A*" in each case. Hence the absolute integrated area of fluorescence by Zn(II) porphyrin which is not bound (free) to plastocyanin in each case was obtained by subtraction of fluorescence of the complex from the observed fluorescence for each of the mixtures, $A_{free} = A_{observed} - A_{complex}$. [c] This value refers to the integrated area of fluorescence. [d] The numbers in parentheses refer to the A_o/A_{free} value determined by using the fluorescence from uncomplexed porphyrin itself when the concentration of quencher (PC) varied as shown in this table.

the wavelength region 375−500 nm. The absorption spectrum of Zn(II)TMPyP^{4+} (5 μM) and the absorption spectrum of the same mixture (5 μM) Zn(II) porphyrin/PC (42.3 μM) which predominantly represent the complex (97.4%) were overlaid in the same figure for comparison. The overlapping band between 425 and 450 nm is indicative of the excitation spectrum to which the absorption spectra of Zn(II)TMPyP^{4+} and of the Zn(II)-TMPyP^{4+}/PC complex are convoluted (Figure 10). This result is in fact supportive of the observation of overlapping fluorescence spectra of the complex and uncomplexed ZnTMPyP^{4+} (632 nm).

Fluorescence Lifetime Measurements. To examine this fluorescence quenching phenomenon in more detail, fluorescence lifetime measurements were performed using the time correlated single photon counting technique on the mixtures of Zn(II)TMPyP^{4+} (5 μM) and PC in the concentration range 0−39 μM. The mixtures of (5 μM) Zn(II)TMPyP^{4+} and PC were excited at 455 nm, and the resulting emission at 632 nm decayed in a biexponential manner as shown in eq 3. At this wavelength of excitation, 455 nm, the predominant absorbing species was the Zn(II)TMPyP^{4+}/PC complex as evidenced by the negative peak at ca. 450 nm in the difference absorption spectra (data not shown). Figure 11 shows the fluorescence decay profiles at 632 nm of the Zn(II)TMPyP^{4+} (5 μM)/PC mixture (39 μM, 97.1% complex) at 25 °C, pH 7.4, 1 mM KCl, and 1 mM phosphate buffer (pH = 7.4) and of the Zn(II)TMPyP^{4+} in the absence of PC. In the absence of PC, the fluorescence decay was single exponential in time with a lifetime of 1.3 ± 0.15 ns. The deconvoluted fitting process of the fluorescence decay profiles of the Zn(II)TMPyP^{4+}/PC mixtures using eq 3 with the IRF yielded two lifetime components for data such as those shown in Figure 11. The biexponential decay fitting in all

$$F = A + B_1 \exp(-t/\tau_1) + B_2 \exp(-t/\tau_2) \qquad (3)$$

mixtures yielded a major lifetime component ca. 1.5−1.4 ns (>88%), which was similar to the observed and reported[39] fluorescence lifetime of Zn(II)TMPyP^{4+}. This lifetime component was assigned as the fluorescence lifetime of the Zn(II)-TMPyP^{4+} that was complexed with the PC, which displays a predominantly static-quenching[21] event that has no effect on the fluorescence lifetime of unassociated Zn(II)TMPyP^{4+} in the absence of diffusional dynamic quenching.[21] The minor fast component (<12%) was weakly resolved, having a comparatively short fluorescence lifetime of 600 ± 300 ps and assigned to another relatively slower static-quenching event originating from a distribution of distances and geometries of the self-associated complexes at the instant of excitation (Table 1).

Discussion

Ground-State Complexation. Recent studies in this laboratory[18,40] of aqueous solutions (pH > 6) containing Pd(II)-TMPyP^{4+} and a pentapeptide composed of four glutamic acid (E) units and one tyrosine (Y) (or tryptophan, W) showed that the four quaternary N atoms of the pyridyl mesosubstituents on the porphyrin framework formed a cationic template in which the carboxylate end groups of the E residues self-assembled to form an ion-pair complex. This served to bring the porphyrin and the Y into proximity in the ground state. Upon photoexcitation of the porphyrin and subsequent generation of its T_1 excited state, ET from the Y to the porphyrin was shown to occur.

It is essential to understand the structural characteristics of the anionic docking site of PC with which the cationic porphyrins are thought to form the self-associated complexes prior to further discussion on the excited-state properties of these complexes. There are two solvent-exposed acidic patches of D and E in the structure of a typical PC in addition to the hydrophobic patch proximate to the Cu atom on the north pole of the protein (Figure 1).[41] In spinach PC, the first acidic patch contains aspartic 42 (D 42), glutamic 43 (E 43), aspartic 44 (D 44), glutamic 45 (E 45), and aspartic 51 (D 51). The second acidic patch of spinach PC consists of glutamic 59 (E 59), glutamic 60 (E 60), and aspartic 61 (D 61) (Figure 1). Moreover, just below this anionic docking surface is a Y83 residue that is solvent-exposed. Obviously it became compelling to investigate whether the same events could be carried out with the PC as with the peptide model system.[18] The first step in this was to ascertain whether the cationic porphyrin would undergo ion-pairing association with the PC. It is well-known that the acidic patch on PC assists docking with its reaction partners, cytochromes *c* and *f* and photosystem I.[34,35] Moreover, the literature contains adequate evidence for ion-pairing interactions between PC and other small molecules. For instance, cationic species such as $[Co(phen)_3]^{3+}$ have been shown to interact with the acidic patch of PC centered on Y83.[33]

Copious evidence for the ionic association is provided by the studies on the ground-state optical absorption spectra of Pd-(II)TMPyP^{4+} and Zn(II)TMPyP^{4+} in the presence of increasing PC content in the mixture. The difference spectra (Figure 3) and the spectrophotometric titrations (Figure 4) show clearly that the presence of the protein influences the electronic properties of the porphyrins, causing the spectra to undergo red-shifting and a decrease of extinction coefficient of the PC/porphyrin complexes. Besides, the similar spectral changes have been reported for mixtures of the same porphyrins with the pentapeptides such as E_4Y.[18] As Figure 5 shows, the same spectral effects occur in mixtures of the cationic porphyrin with an oligo-glutamic acid (peptide) containing an average of 7 E

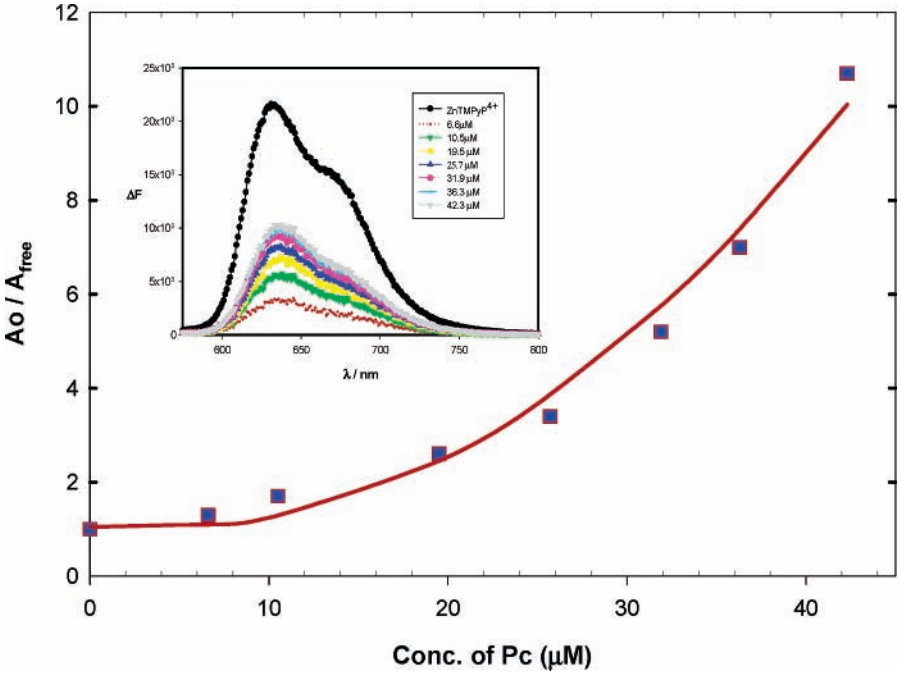

Figure 9. Modified Stern−Volmer plot of ratio of integrated area of fluorescence A_o/A_{free} versus the concentration of plastocyanin at 25 °C, pH = 7.4, and at 1 mM KCl, 1 mM phosphate buffer (pH = 7.4). $A_{free} = A_{observed} - A_{complex}$ and $A_{complex} = A_{difference\ fluorescence} \times$ % complexation. The solid line is the calculated fit according to eq 1 for $k_{sv} = 1.9 \times 10^4\ M^{-1}$, where $\beta = 1$. Inset: Difference fluorescence spectra obtained by subtraction of the spectra obtained after mixing (5.0 μM Zn(II)TMPyP^{4+}/plastocyanin complexes for the mixtures in the concentrations 6.6, 10.5, 19.4, 25.7, 31.9, 36.3, and 42.3 μM of plastocyanin) from that obtained before mixing (pure Zn(II)TMPyP^{4+} fluorescence). The black spectrum is for the pure Zn(II)TMPyP^{4+}. Each solution is in 1 mM KCl and 1 mM phosphate buffer (pH = 7.4) at 25 °C.

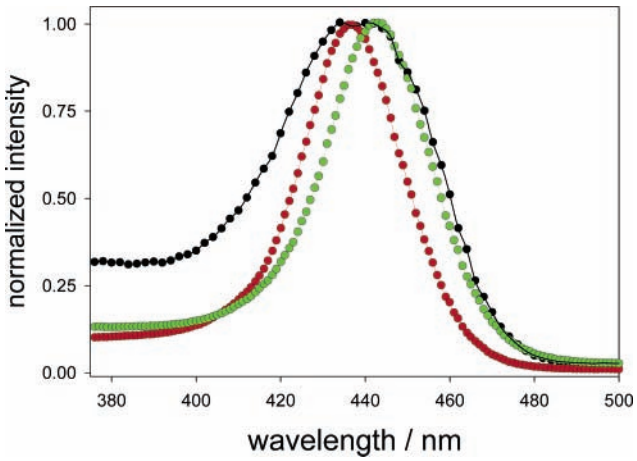

Figure 10. Excitation spectrum of 5 μM Zn(II)TMPyP^{4+}/42.3 μM plastocyanin obtained by monitoring the fluorescence at 632 nm over the excitation range 250−600 nm. Only the spectrum in the wavelength range 375−500 nm is shown. The absorption spectrum of Zn(II)-TMPyP^{4+} (5 μM) and that of the 5 μM Zn(II)TMPyP^{4+}/42.3 μM plastocyanin were overlaid in the same plot.

units per molecule as well. Since comparable spectral changes (intensity decrease and the red-shifts) happen in the presence of the protein and in the two oligo-peptide cases and the only common factor in all three cases is a patch of negative charge, it can be clearly concluded that the association between the cationic MPs and PC occurs at the acidic patch, in which case the porphyrin is placed proximate to Y83. A further conclusion rising out of the oligo-Glu experiment is that the MP−PC association does not require the presence of a nearby tyrosine. However, the presence of Y83 may enhance the binding interactions between the cationic porphyrins and anionic docking site of PC. Furthermore, the observed association constant on the binding between Y83 mutant plastocyanin (Y83F-PC) and Pd(II)TMPyP^{4+} ($K = 7.0 \times 10^4\ M^{-1}$) is appreciably lower by a factor of 11.5 than that for the native PC and Pd(II)TMPyP^{4+} system [$K = (8.0 \pm 1.1) \times 10^5\ M^{-1}$]. The substitution of Y83 with F eliminates the possibility of coordination to the Pd(II) center as predicted in the Y83-assisted self-association of Pd-(II)TMPyP^{4+} to PC. Thus, these results imply that the solvent-exposed Y83 residue of the self-associated cationic porphyrin/PC complexes is indeed involved in the binding interaction between the two reaction partners.

Ligation of Y83 with MP/PC Complexes. Consequently, it is deemed necessary to understand the nature of the interaction that results in this Y83-assisted ion association between the cationic porphyrins and PC. The decrease of ground-state extinction coefficients of the complexes and concomitant red-shift of the Soret band and the Q-bands of these Y83-assisted self-associated complexes with the addition of PC can be explained in terms of the "theory of charge transfer". If an electron acceptor and an electron donor form a complex displaying the electronic interactions between the components, a new absorption band is commonly observed.[42] This band is known as a charge−transfer band and possesses characteristic features different from either the donor or the acceptor. It is attributed to a donor−acceptor complex formed by the partial or complete transfer of an electron from a donor to an acceptor. Additionally, for a number of irregular porphyrins (e.g., Pd(II) porphyrin), the excited singlet states are too short-lived ($\tau \leq 1$ ns), and photochemical reactions may occur efficiently when there is some interaction between the porphyrin and the quenchers in the ground-state itself. Hence, the reversible[39] binding of the ligands at the vacant axial positions of the MPs is a possible process. Also, Zn^{2+} and Pd^{2+} are known to have extended square pyramidal geometry for the biological ligand, a tyrosine.[43] Tyrosine is known[43] as a biological ligand to which specific metal ions selectively bind as well. For instance, in the protein transferrin[43,44] the iron (Fe^{3+}) at the N-terminal iron-binding domain is bound by two tyrosines (as well as a histidine

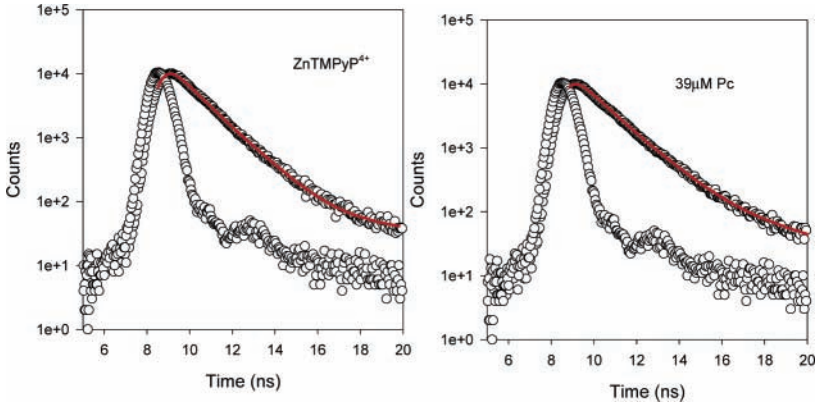

Figure 11. Fluorescence time profiles (time-correlated single photon counting) of the 632 nm luminescence of Zn(II)TMPyP^{4+} (5 μM)/plastocyanin mixture (39 μM) (left panel) and of Zn(II)TMPyP^{4+} (5 μM) at 25 °C, pH = 7.4, 1 mM KCl, and 1 mM phosphate buffer (pH = 7.4). The instrumental response function is shown with each decay profile.

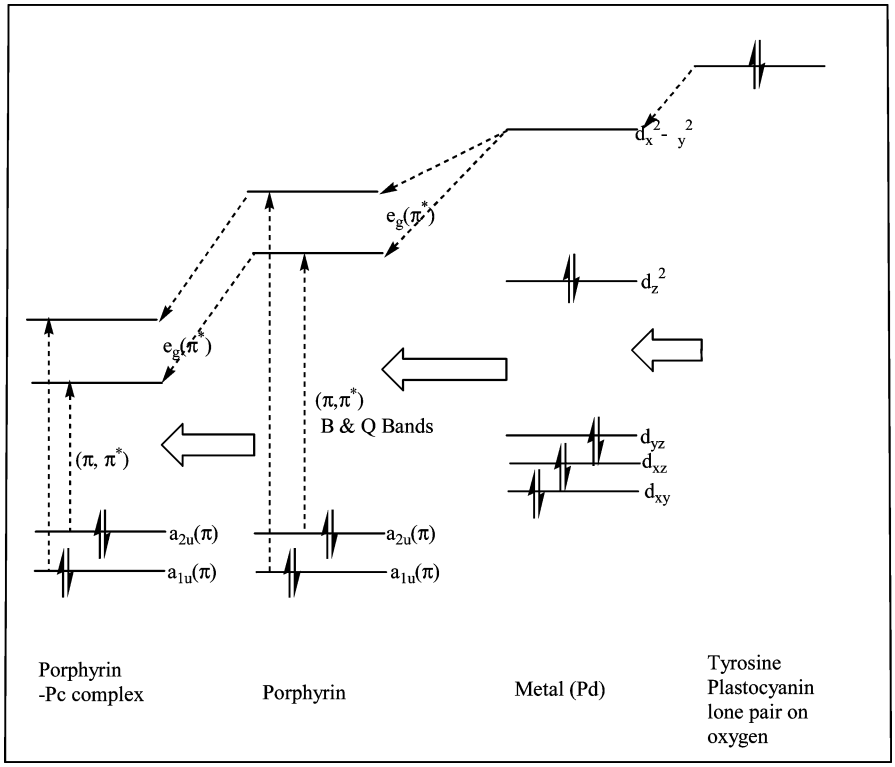

Figure 12. Energy level diagram to demonstrate the interaction of the tyrosine residue of plastocyanin with the metalloporphyrin ring to produce the porphyrin−plastocyanin complex.

and an aspartic acid) in the presence of CO_3^{2-} ions, and the red color of the Fe^{3+} protein arises from a tyrosinate → Fe^{3+} charge-transfer transition.

Moreover, the MD calculation provides adequate evidence for the proximity of the center of mass of porphyrin and the center of mass of the phenolic ring of the Y83 residue located just beneath the anionic surface docking site of self-associated PC (5−9 Å) described in the current studies. Thus, similar types of charge-transfer interactions are indeed predictable between the hydroxyphenyl terminus of Y83 residue and the Pd(II) and Zn(II) metal centers of the self-assembled cationic porphyrins/PC complexes. The red-shift of the bands (Soret and Q) of the complexes may then be attributed to the capability of Y83 to assist the binding by coordinating as an axial ligand to the metal centers thereby forming a charge-transfer band. However, the experiments were carried out at pH 7.4, and the pk_a of tyrosine is 9.3, so it is most likely to be protonated under these conditions. Therefore, a partial transfer of charge from the nonbonding lone pair of oxygen atoms of the hydroxyphenyl terminus of Y83 moiety to the metal centers of porphyrins would be more favorable in the self-assembled complexes.

Thus, the coordination of hydroxyphenyl terminus of Y83 residue as an axial ligand to the metal centers, Pd(II) and Zn(II) of the PC/porphyrin complexes is intriguing and can be understood from a molecular point of view. Furthermore, this charge-transfer ligation is attributed to the observed decrease of extinction coefficients of the cationic porphyrins/PC system with a gradual red-shift (ca. 9 nm for Pd(II) system and ca. 6 nm for Zn(II) system) of the Soret and Q-bands of the current self-associated complexes. This mechanism can be explained in terms of the so-called four-orbital model developed by Gouterman[39,45] et al. for the interpretation of UV−vis spectra and luminescence properties of porphyrins, coupled with the molecular exciton model[46] (Figure 12, energy level diagram).

Kasha[46] defined the exciton model for the resonance interaction between the excited states of weakly-coupled molecular

systems. This model describes the intermolecular interaction in a molecular aggregate as a sum of multipoles (dipole−dipole, quadrapole−quadrapole, etc.). If a pair of degenerate dipolar states on one chromophore interacts with a similar pair on the other chromophore, the nature of exciton coupling and the energy of the resulting exciton states will depend on the dimer geometry (interchromophore distance).[47,48] If the newly formed complex involves an electron acceptor and an electron donor with electronic interactions between the components, a new absorption band, a charge-transfer band, is usually observed.[42,49] This charge-transfer band is associated with a donor−acceptor complex formed by the partial or complete transfer of an electron from donor to acceptor.[50,51]

Thus, the filled nonbonding orbital of the oxygen atom of the hydroxyphenyl terminus on Y83 moiety can be located at the energies above the empty $e_g(4d_{x^2-y^2})$ of Pd(II) ion of the virtual spectrum, and it will be pushed down in energy as a result of bonding with the oxygen lone pair on the Y83−hydroxyphenyl terminus, a mode that can be described as a charge-transfer bonding interaction (Figure 12). The simultaneous bonding interaction of this state, $e_g(4d_{x^2-y^2})$, with the empty $e_g(\pi^*)$ state will stabilize the $e_g(\pi^*)$ state further, resulting in red-shifted B and Q-bands for the porphyrin−PC complex. The electric dipole selection rules for the final transition to these states of the complex govern the extinction coefficients for these transitions. If the transitions are symmetry forbidden, then a decrease of extinction coefficient of the system should be expected.

The similar diagram can be proposed for the ligation interaction of Y83 with the Zn(II) metal ion and the simultaneous interactions in the self-associated Zn(II)TMPyP^{4+}/PC system. The Gouterman model[39,45] itself accounts for the difference of electronic configurations and crystal field energies of MPs. Accordingly, Zn(II) porphyrin belongs to the class of regular porphyrins with a closed shell central metal atom ($3d^{10}$). Thus, the interaction of the porphyrin π macrocycle with the central metal is negligibly small, and thereby red-shifted Q and B bands (regular porphyrins) are usually observed compared to those of Pd(II) porphyrins (irregular porphyrins). Additionally, the lowest unoccupied molecular orbital (LUMO) of Zn^{2+} in Zn(II)TMPyP^{4+} is a 4S orbital, and perhaps this orbital can be regarded as the empty orbital with the correct symmetry and acquired energy to which the oxygen-lone pair of hydroxyphenyl terminus of Y83 residue is donated. However, these proposed ligation interactions should be tested by quantum mechanical calculations, and further work on refining this diagram (Figure 12) will be in progress.

Job's Plots. The data from the spectrometric titrations have been analyzed using Job's method[29] to determine the stoichiometry of the complexes and their stability. The plots shown in Figures 3, 6, and 7 for Pd(II)TMPyP^{4+} and Zn(II)TMPyP^{4+} (data not shown) indicated that the observed difference spectra arise from the *predominant* formation of a 1:1 self-association complex between cationic porphyrins and anionic surface docking site of the PC,

$$\mathrm{M(II)TMPyP^{4+}} + \mathrm{PC} \rightleftharpoons \mathrm{M(II)TMPyP^{4+}{:}PC}$$

where M = Pd or Zn. With all the evidence from the ground-state spectral studies and MD calculations along with relevant literature,[52] it is clear that the major factor responsible for the complex formation is the electrostatic interaction between 4+ charges of the porphyrins and anionic aspartic acid and glutamic acid patch of the protein. Also, the selected low concentration of ionic strength buffer (1 mM KCl) yields a self-associated complex of higher stability.[17] There are several important features displayed in the Job's diagrams. Figure 6 shows a plot resulting from a Job's treatment of the spectrophotometric titration data for PC and Pd(II)TMPyP^{4+}. A similar diagram was obtained for the Zn porphyrin/PC case. The plot shows a minimum corresponding to the 1:1 stoichiometry of the complex as evidenced by the utmost departure, $F(x)$, at which the molar fraction of each component, Pd(II)TMPyP^{4+} and PC, is 0.5 . However, the minimum is not very sharp,[30] and the linearity of the data at low protein concentrations is barely smeared. In this region the first few aliquots of protein are being added, and the molar fraction of porphyrin is in great excess of that of the PC in which the ratio of molar fraction of metalloporphyrin to PC, $M_{MP}/M_{PC} \gg 1$. Under these conditions ($M_{MP}/M_{PC} > 1$), there is a formation of an intermediate complex of 4:1 composition of which an association of four porphyrin molecules with one PC molecule (there are two acidic patches on PC, the second on the western face) was also seen (Figure 6). But the equilibrium-binding constant of formation of these complexes must be extremely low as reflected from a very blunt point ($M_{MP} = 0.8$) for formation of such complexes (Figure 6). Then, as the concentration of PC was increased the equilibrium would shift to favor a thermodynamically more stable 1:1 complex. Besides, in the concentration region where $M_{MP}/M_{PC} \ll 1$, the data are much better represented by the 1:1 line. This is the concentration region (more than 80−97% porphyrin in complexed form) where all the photoexcitation experiments described in this paper and in the succeeding paper were carried out. In addition, the calculation of concentration of protein is firmly dependent on the method used, and possible errors in the evaluation of PC concentration by the value of the extinction coefficient of tyrosine ($1.4 \times 10^3\ M^{-1}\ cm^{-1}$)[26] may also account for the departure from linearity of the Job's plots at very low levels of concentration of protein ($M_{MP}/M_{PC} \gg 1$), since this method does not take into account the environmental influence[26] on the extinction coefficient of the tyrosines present in different positions of the structure of PC (Figure 1, partially solvent-exposed Y70, completely buried inside the protein Y80, and solvent-exposed Y83). The MD calculation of the self-assembled PC and porphyrin complexes is also supportive of the formation of docking complexes with 1:1 stoichiometry as well. Moreover, the encouraging evidence for the formation of a thermodynamically stable 1:1 self-associated complex was provided by the spectrometric titration data fitted to an excellent nonlinear fit such as shown in Figure 7 for the Pd(II)TMPyP^{4+}/PC complex, in which case the equation (vide supra) was derived for a complex formation with 1:1 stoichiometry. Besides, spectrometric titration data fitted to a nonlinear fit such as shown in Figure 7 has been taken as evidence for the formation of complexes with 1:1 stoichiometry in the case of cationic lysine peptides and an anionic patch of PC system, and no Job's plots have been reported.[53]

Binding Constants. The binding constants of the two complexes were calculated to be high on the order of ca. $10^6\ M^{-1}$. Moreover, the binding constant for Zn(II)TMPyP^{4+}/PC complex was alternatively obtained from the fluorescence data presented in the modified Stern−Volmer plot of Figure 9. The binding constant thus evaluated from the regression parameters of the nonlinear curve fit (Figure 9) by means of eq 1 was (3.5 ± 0.8) $\times 10^5\ M^{-1}$, a factor of ca. 7 lower than that obtained by UV−vis spectrometric titration data. The ambiguity of the manual deconvolution of the fluorescence data into the fluorescence of the complex and of the uncomplexed porphyrin

accounts exclusively for this difference. Additionally, in the extraction of binding constant from the regression parameters, $\beta = 1$ was assumed for optically dilute solutions (eq 1). Nonetheless, the optical dilution of the mixtures of Zn(II)-$TMPyP^{4+}$/PC was not ideal due to the trace of turbidity often typically present in protein solutions, and thus the exact value for β should also be taken into account to ascertain a closer agreement in the two methods.

The binding constants of significantly high magnitude are attributed in part to the very low concentration of ionic strength (1 mM KCl) buffer used in all of the experiments.[17] The coordination of Y83 as a fifth ligand to the metal centers in the self-associated porphyrin/PC complexes (vide supra) may indeed account for the observed considerably larger binding constants as well. The spectrometric binding studies between PC and the freebase H_2TMPyP^{4+} in which no central metal ion is present, yielded a binding constant of $K = 3.5 \times 10^5\ M^{-1}$, a factor of ca. 3 lower than the Pd(II) porphyrin/PC case, and thus provides supportive evidence for the above argument. In addition, our spectrometric binding studies on the Y83F-PC/Pd(II)$TMPyP^{4+}$ system determined a binding constant of a factor of 11.5 lower than that of the plastocyanin/Pd(II)$TMPyP^{4+}$ complex, confirming Y83-assisted binding and hence the cause for the higher binding constants in such cases as well. Furthermore, the role of acidic residues of PC in its interaction with cytochrome *f* has been studied by Bendall et al.,[36] who reported a binding constant of $1.4 \times 10^3\ M^{-1}$ for the interaction of Cyt *f* and Y83 mutant PC (Y83F) in which Y83 was substituted by a F residue and a value of 1 order of magnitude higher ($1.0 \times 10^4\ M^{-1}$) for the same interactions with wild-type spinach PC.

The binding constant in Pd(II)$TMPyP^{4+}$/PC complex is smaller by a factor of 3.3 than that of Zn(II)$TMPyP^{4+}$/PC complex. The difference of magnitudes of binding constants in the two cases can be explained in terms of hard and soft acid and bases (HSAB) theory.[43,54] Accordingly, when tyrosine (hard ligand) binds to the Pd^{2+} (soft) center in the Pd(II)$TMPyP^{4+}$ molecule as a fifth ligand, the resulting complex would be less stable [$K = (8.0 \pm 1.1) \times 10^5\ M^{-1}$] than the complex formed by combination of Zn^{2+} (intermediate) and tyrosine [$K = (9.86 \pm 1.1) \times 10^5\ M^{-1}$].[43,54]

Fluorescence Studies. The UV−vis absorption difference spectra and spectrometric binding studies along with Job's plots showed that under the solution conditions of those shown in Figures 3, 4, and 7 the zinc(II) porphyrin is also present in a 1:1 stoichiometric-association complex (data not shown) with PC [$K = (2.7 \pm 0.8) \times 10^6\ M^{-1}$ in 1 mM KCl, 1mM phosphate buffer, pH = 7.4]. Such self-association is found between cytochrome *c* and PC[55] and other protein−protein[56] systems (e.g., cytochrome *c* and cytochrome b_5 and flavodoxin). Besides, the photoexcitation of Pd(II)$TMPyP^{4+}$ does not yield fluorescence since the intersystem crossing from the S_1 state is exceedingly rapid and has been reported as restricting S_1 lifetimes to ca. 20 ps.[39] Nevertheless, the excitation of Zn(II)-$TMPyP^{4+}$ into its S_1 state by Q-band irradiation yields fluorescence in the 600−750 nm spectral region ($^{em}\lambda_{max} = 632$ nm) (Figure 8). Excitation of Zn(II)$TMPyP^{4+}$/PC mixtures into the singlet state by 550 nm at the edge of the Q-band irradiation in which the absorption by the Zn(II)$TMPyP^{4+}$/PC complex was predominant over that of Zn(II)$TMPyP^{4+}$ yielded the fluorescence intensity quenching (Figures 8 and 9) at low ionic strength (1 mM KCl). The evaluated Stern−Volmer constant K_{sv} extracted from the linear plot (inset of Figure 8) was $1.9 \times 10^4\ M^{-1}$. Taking the measured lifetime of 1.3 ns for the singlet state[57] of Zn(II)$TMPyP^{4+}$ leads to a bimolecular reaction rate constant of $1.5 \times 10^{13}\ M^{-1}\ s^{-1}$ for the quenching of the porphyrin fluorescence. This is far in excess of the value for a rate constant of a diffusion-controlled process in aqueous solution, and it serves to indicate that the fluorescence intensity quenching is not just a dynamic event but must arise predominantly from an associational static-quenching process caused by the proximity of the components (porphyrin/PC) at the instant of excitation.[58] The formation of self-associated complexes in which the metal centers of the porphyrin molecules were presumably coordinated by Y83 as an axial ligand in the ground-state (vide supra) as well as the MD calculation on such complexes did indeed provide the evidence for the proximity of the porphyrin− PC couple (Table 1, the shortest calculated inter-chromophore distance is ∼5.5 Å) for this static quenching process to occur.

Fluorescence Spectra of the Complex and Static Fluorescence Quenching. Scrutiny of Figure 8 leads to the interesting observation that at the highest concentration of PC (42.3 μM) in which more than 97% of the zinc porphyrin molecules are present in complexed form, the quenched fraction has leveled out at close to 50%. Interestingly, the constructed difference fluorescence spectra (inset to Figure 9) predominantly represent the fluorescence spectra of the complex and display bands centered at 635 nm, ca. 3 nm red-shifted compared to that of uncomplexed Zn(II)$TMPy^{4+}$ (632 nm). The band intensity of these fluorescence maxima increases with the concentration of PC and levels off at the most predominant complexation. Thus, it is revealed that the fractional fluorescence quenching (50%) at the most predominant complexation, in which 97.4% of Zn-(II) porphyrin molecules are in complexed form, is due to the ground-state formation of a strongly fluorescent preformed complex of which the fluorescence spectrum overlaps with that of the uncomplexed Zn(II)$TMPyP^{4+}$ (inset of Figure 9). Moreover, the modified Stern−Volmer plot (Figure 9) generated upon subtraction of the residual fluorescence of the complex was nonlinear with upward-curvature from which the evidence for the predominant static quenching[20,21] in the presence of diffusional-dynamic quenching was revealed exactly as described by eq 1, presumably by the Y83 moiety of the self-associated complex. Indeed, our flash photolysis kinetic studies between Y83F-PC and the Pd(II)$TMPyP^{4+}$ system that are described in the succeeding paper are clearly supportive of the evidence for the Y83-mediated electron-transfer processes in the triplet state as well. Interestingly, upon subtraction of the residual fluorescence of the complex, the percentage of fluorescence intensity quenching reaches the percentage of complexed porphyrin (Table 3, Figure 9). These data are consistent with previous studies in which the evidence for both static and dynamic quenching (depending on the extent of complexing) for the complexes of this type in aqueous media has been documented.[59] In the case of $Ru(phen)_2(CN)_2$, the fluorescence of this molecule has been reported[60] to be quenched by Ni^{2+}-(static quenching) by coordination to the CN^-, which acts as a bridging ligand. Additionally, this result is also similar to the experimental results reported previously by Logunov et al.[59c] for the $MTMPyP^{4+}$ and AQS (9,10-anthraquinone disulfonate derivatives) self-assembled system. A nonlinear upward-curved Stern−Volmer plot was reported for the quenching of the fluorescence arising from uncomplexed porphyrin considering that all the complexes between $MTMPyP^{4+}$ and AQS were nonfluorescent with a combination of 1:1 or 1:2 stoichiometry. The current result is substantiated by the results of single-photon counting measurements in which an unquenched fluorescence lifetime component of 1.3 ns was resolved for the static

SCHEME 1: Proposed Scheme for the Singlet State Processes of Zn(II)TMPyP^{4+}/Plastocyanin Complex[a]

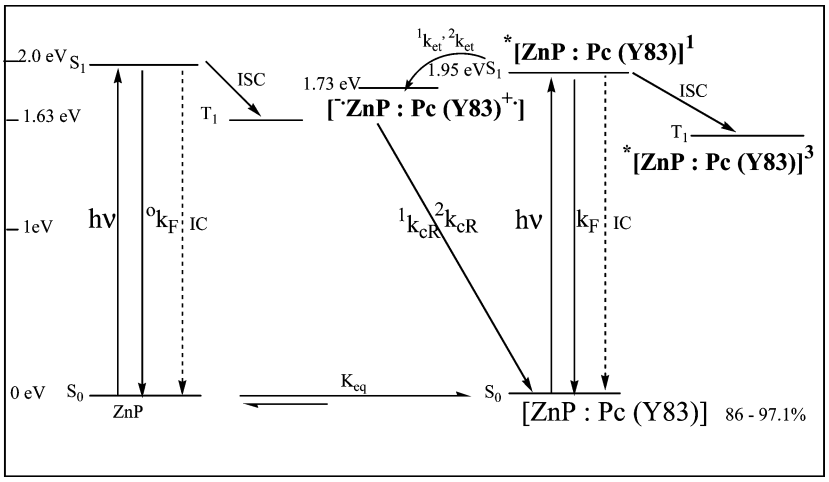

[a] The energy of each state of the uncomplexed porphyrin was adapted from ref 39 and the average energy of the complex was taken from the molecular-dynamic calculation.

quenching event associated with the complexed Zn(II)TMPyP^{4+} (vide supra).[20,21]

Moreover, the decreased quantum efficiency of the complex (50%) can be understood in terms of the porphyrin S_1 state being presented with another nonradiative deactivation channel under complexation conditions (Scheme 1).The nature of the additional deactivation event when the porphyrin is complexed is uncertain, but it can be understood that it occurs as a result of an electron-transfer event originating from the Y83 moeity of the self-associated complex (Scheme 1) and happening at the instant of excitation (ca. within a few femtoseconds time).

Mechanism of Fluorescence Quenching. The observed concept of fluorescence quenching, presumably by the self-associated Y83 moiety, is intriguing and can be understood in terms of the driving force for the electron-transfer process. The MD calculations show that when complexed the center of mass of the porphyrin is located between 5 and 12 Å, average near 9 Å, from the center of mass of the hydroxyphenyl terminus of the solvent-exposed Y83 residue on the nearby strand. At pH 7, the driving force for an ET between the singlet state of the Zn porphyrin and tyrosine (refers to the Y83 located just below the anionic arch) is calculated to be ca. 0.20 V by taking the redox potential for the singlet state of Zn(II)TMPyP^{4+} as 1.13 V[57] and the reduction potential of the tyrosine radical cation at pH 7 as 0.93 V.[61] Hence the singlet state electron-transfer process will be favorable by 0.2 eV. Even though the driving force for ET from the singlet state is not significantly large, the electron-transfer processes are rapid enough to compete with the intrinsic decay process of Zn(II)TMPyP^{4+} by which a relatively short fluorescence lifetime of 1.3 ns is determined (Scheme 1).[57] Thus, the proximity of the preformed porphyrin−PC couple by Y83-assisted self-association (distribution of distances from ca. 5 to 8 Å) as well as the favorable driving force on the ET in the singlet state does indeed yield fast electron-transfer fluorescence quenching (static).

Fluorescence Lifetime Measurements. We turn now to the single-photon counting luminescence measurements of the Zn(II)TMPyP^{4+} and PC mixtures; the excitation was carried out at 455 nm, close to the falling edge of the porphyrin-like absorption of the preformed [Zn(II)/PC] complex. At this wavelength of excitation, 455 nm, the predominant absorbing species was the Zn(II)TMPyP^{4+}/PC complex as evidenced by the negative peak at ca. 450 nm in the difference absorption spectra (data not shown). Thus, at the concentration range used (0−39 μM and 0−97% complexation) the predominant emitting species was the excited state of the complex with residual emission from uncomplexed porphyrin at 632 nm. Therefore, it is clear that both the complex and the free uncomplexed porphyrin contribute to the fluorescence decay profile and that the major component of the decay should be attributed to the fluorescence of the complex. Indeed, the time-correlated single-photon counting measurements showed a major (>88%) longer-lived fluorescence component having a lifetime of 1.4 ± 0.15 ns assigned to the static quenching event having arisen from the Y83 moiety of the self-associated complex; with Zn(II)-TMPyP^{4+} alone in buffer solution at pH 7.4 (Figure 11) this was the sole component. Thus, the major concentration-independent unquenched fluorescence lifetime value was assigned to the static fluorescence quenching[20,21] originating from the singlet state of the preformed self-associated Zn(II)-TMPyP^{4+}/PC complex, in which the metal center Zn(II) is coordinated by the hydroxyphenyl terminus of Y83 moiety in the ground-state ($^1k_{et}$, Scheme 1). An approximate value for the weakly resolved shorter-lived component (<12%) was 600 ± 300 ps, taken as an average of three experiments at different PC concentrations of 0−39 μM. This component is regarded as having originated from a different, relatively slower static quenching event associated with the presence of distribution of distances and orientations of porphyrin/PC complexes at the instant of excitation ($^2k_{et}$, Scheme 1). Besides, this evidence is supported by the MD calculation in which an assembly of geometries and distances of porphyrin/PC complexes was shown to be formed at the last 30 ps of the simulation procedure (Table 1). Also, the time resolution of the single-photon counting instrument developed in our laboratories was ca. 700 ps on the basis of IRF analysis. Thus, the IRF of the single-photon counting instrument was insufficient to precisely resolve lifetime components that are very close (e.g., 1.4 ± 0.15 ns and 600 ± 300 ps), and consequently the faster fluorescence lifetime component and the pre-exponential factor were subjected to a significant error. Even if the probability of the second static-quenching process is comparatively less with increased complexation (data not shown), the rate constant of ET for this process was readily determined. As discussed above, if the electron-transfer process is responsible for the deactivation of the S_1 state of the complex (in equal competition with the other radiative and nonradiative channels), the rate constant of ET associated with the second process (Scheme 1) was determined to be $^2k_{et} = (1.1 \pm 0.6) \times$

10^9 s^{-1}. This rate was calculated by the equation $^2k_{et} = 1/\tau - 1/\tau_o$, where τ is the average of quenched fluorescence lifetime observed at different PC concentrations of 0−39 μM ($\tau = 600 \pm 300$ ps) and τ_o is the fluorescence lifetime of the free (unassociated) Zn(II)TMPyP^{4+}. In addition, the experimentally evaluated rate constant of ET for the singlet state quenching of Zn(II)TMPyP^{4+}/PC complex, $^2k_{et}$, agrees well with the electron-transfer rate constant calculated on the Marcus model[62] (1.9×10^9 s^{-1}) for typical protein mediated electron-transfer parameters ($\lambda = 1$ eV, $\beta = 0.9$ Å^{-1}).[40,52,62] Nevertheless, the determination of overlap parameter β and the proper assignment on the singlet state electron-transfer process of the complex are indeed necessary, and experiments are thus underway to measure these electron tunneling parameters as will be discussed in the succeeding paper. The study of the faster intramolecular electron-transfer process (Scheme 1, $^1k_{et}$) from the singlet state of the complex, which arises due to associational static quenching, may require ultrafast techniques and will be suited for further studies of the singlet state of the complex.

Proposed Scheme for the Singlet State Processes. The final point of concern is to discuss the mechanistic scheme for the singlet state processes described above. The various processes involving zinc porphyrin and PC are shown in Scheme 1. Because of the overall charges of Zn(II) porphyrin (Zn(II)P) and PC at pH 7.4 are +4 and −8, respectively, the porphyrin and the protein readily associate. At the selected very low ionic strength (1 mM) the kinetic regime is adjusted to predominately unimolecular (to the right-hand side of the equilibrium) because of the strong binding constant for the association. The unimolecular mechanism is described as follows. Excitation of zinc porphyrin (Zn(II)P) associated with PC produces the singlet state of the preformed complex, S_1, *[ZnP:PC(Y83)]^1. This is followed by the fluorescence of the complex (k_F) in equal competition with the other pathways on the decay of the complex, the two electron-transfer processes, $^1k_{et}$ and $^2k_{et}$, (k_{CR}, charge recombination) originating from the distribution of the geometries/distances of the complex, internal conversion (IC) and intersystem crossing (ISC) to produce the triplet state of the complex, T_1, *[ZnP:PC(Y83)]^3. In this scheme, the transient species arising from this distribution was not yet differentiated in terms of the energy. Moreover, the ultrafast studies of the complex will be more beneficial in terms of further investigation of the charge recombination steps ($^1k_{CR}$, $^2k_{CR}$) and the transient species for the electron-transfer processes such as shown in the Scheme 1. The deactivation of the singlet state of the fraction of uncomplexed porphyrin by all possible nonradiative pathways in competition with the radiative fluorescence decay ($°k_F$) is shown in the left panel of Scheme 1.

In conclusion, we have demonstrated that the cationic porphyrins Pd(II)TMPyP^{4+} and Zn(II)TMPyP^{4+} form self-associated complexes with the anionic-solvent exposed asparate (D) and glutamate (E) patch of PC in the ground-state in 1 mM KCl buffer at pH = 7.4 and 25 °C. The ground-state spectrometric binding studies, Job's plots, along with the MD calculation revealed the predominant formation of preformed complexes of 1:1 stoichiometry with significantly high binding constants. The steady-state and time-resolved fluorescence studies of the self-associated Zn(II)TMPyP^{4+}/PC complex showed the singlet-state quenching of Zn(II) porphyrin by a static mechanism (ET) and revealed the formation of a significantly fluorescent complex in the ground-state as well. Also, the Y83 moiety of the self-associated complexes was implicated in binding and in these electron-transfer processes as evidenced by the experiments conducted on Y83F-PC.

Acknowledgment. This research has been supported in part by the National Institutes of Health, Grant No. CA91027 and by the Center for Photochemical Sciences at Bowling Green State University. H.M.A. is grateful to the McMaster Foundation at Bowling Green State University for a fellowship. The authors wish to acknowledge Dr. Michael Y. Ogawa and Dr. A. Gusev, Department of Chemistry & Center for Photochemical Sciences at Bowling Green State University, for useful scientific discussions throughout this project.

References and Notes

(1) Rabinowitch, E. I. *Photosynthesis;* Wiley: New York, 1951; Vol. 2.
(2) Chang, C. K. *J. Am. Chem. Soc*. **1977**, *99*, 2819.
(3) Zaleski, J. M.; Chang, C. K.; Nocera, D. G. *J. Phys. Chem.* **1993**, *97*, 13206.
(4) Harriman, A.; Odobel, F.; Sauvage, J. P. *J. Am. Chem. Soc.* **1994**, *116*, 5481.
(5) Hudson, M. F.; Smith, K. M. *Tetrahedron* **1975**, *31*, 3077.
(6) Nikolaitchik, A. V.; Korth, O.; Rodgers, M. A. J. *J. Phys. Chem. A* **1999**, *103*, 7587.
(7) Gusev, A. V.; Rodgers, M. A. J. *J. Phys. Chem A* **2002**, *106*, 1985.
(8) Kimura, A.; Funatsu, K.; Imamura, I.; Kido, H.; Sasaki, Y. *Chem. Lett*. **1995**, 207.
(9) Di Bilio, A. J.; Dennison, C.; Gray, H. B.; Ramirez, B. E.; Sykes, A. G.; Winkler, J. R. *J. Am. Chem. Soc*. **1998**, *120*, 7551.
(10) Jackman, M. P.; McGinnis, J.; Powls, R.; Salmon, G. A.; Sykes, A. G. *J. Am. Chem. Soc*. **1988**, *110*, 5880.
(11) Sigfridsson, K.; Ejdeback, M.; Sundahl, M.; Hansson, O. *Arch. Biochem. Biophys*. **1998**, *351*, 197.
(12) Meade, T. J.; Gray, H. B.; Winkler, J. R. *J. Am. Chem. Soc*. **1989**, *111*, 4353.
(13) (a) Balbinot, D.; Atalick, S.; Guldi, D. M.; Hatzimarinaki, M.; Hirsch, A.; Jux, N. *J. Phys. Chem. B* **2003**, *107*, 13273. (b) Tran-Thi, T. H.; Gaspard, S. *Chem. Phys. Lett*. **1988**, *148*, 327. (c) Segwa, H.; Nishino, H.; Kamikawa, T.; Honda, K.; Shimidzu, T. *Chem. Lett*. **1989**, 1917. (d) Shimidzu, T.; Iyoda, T. *Chem. Phys. Lett*. **1981**, 853.
(14) (a) Zhou, J. S.; Kostic, N. M. *J. Am. Chem. Soc*. **1991**, *113*, 6067. (b) Zhou, J. S.; Kostic, N. M. *J. Am. Chem. Soc*. **1991**, *113*, 7040. (c) Zhou. J. S.; Kostic, N. M. *J. Am. Chem. Soc*. **1992**, *114*, 3562 (d) McLendon, G.; Miller, J. R. *J. Am. Chem. Soc*. **1985**, *107*, 7811. (e) McLendon, G.; Conklin, K. T. *J. Am. Chem. Soc*. **1988**, *110*, 3345. (f) Hirota, S.; Hayamizu, K.; Okuno, T.; Kishi, M.; Iwasaki, H.; Kondo, T.; Hibino, T.; Takabe, T.; Kohzuma, T.; Yamauchi, O. *J. Am. Chem. Soc*. **1998**, *120*, 8177. (g) Qin, L.; Kostic, N. M. *Biochemistry* **1993**, *32*, 6073.
(15) (a) Crnogorac, M. M.; Shen, C.; Young, S.; Hansson, O.; Kostic, N. M. *Biochemistry* **1996**, *35*, 16465.
(16) (a) He, S.; Modi, S.; Bendall, D. S.; Gray, J. C. *EMBO J*. **1991**, *10*, 4011.
(17) Zhou, J. S.; Granada, E. S. V.; Leontis, N. B.; Rodgers, M. A. J. *J. Am. Chem. Soc*. **1990**, *112*, 5074.
(18) Aoudia, M.; Rodgers, M. A. J. *J. Am. Chem. Soc*. **1997**, *119*, 12859.
(19) (a) Hirota, S.; Hayamizu, K.; Endo, M. T.; Hibino, T.; Takabe, T.; Khzuma, T.; Yamauchi, O. *Biochemistry* **2000**, *39*, 6357. (b) Clark-Ferris, K. K.; Fisher, J. *J. Am. Chem. Soc*. **1985**, *107*, 5007. (c) Modi, S.; Nordling, M.; Lundberg, L. G.; Hansson, O.; Bendall, D. S. *Biochim. Biophys. Acta* **1992**, *1102*, 85. (d) He, S.; Modi, S.; Bendall, D. S.; Gray, J. C. *EMBO J*. **1991**, *10*, 4011.
(20) (a) Balzani, V.; Moggi, L.; Manfrin, M. F.; Bolletta, F. *Coord. Chem. Rev*. **1975**, *15*, 321. (b) Demas, J. N.; Addington, J. W. *J. Am. Chem. Soc*. **1976**, *98*, 5800.
(21) Demas, J. N. *Excited-State Lifetime Measurements;* Academic Press: New York, 1983.
(22) Heinlein, T.; Knemeyer, J.; Piestert, O.; Sauer, M. *J. Phys. Chem. B* **2003**, *107*, 7957.
(23) Ellefson, W.; Ulrich, E.; Krogmann, D. W. *Methods Enzymol*. **1992**, *69*, 223.
(24) Ashton, A.; Anderson, L. *Biochem. J*. **1981**, *193*, 375.
(25) Krogmann, D. W.; Morand, L. Z. *Biochim. Biophys. Acta* **1993**, *1141*, 105.
(26) Copeland, R. A.; *Methods for Protein Analysis;* Chapman & Hall: New York, 1994.
(27) (a) Babu, C. R.; Volkman, B. F.; Bullerjahn, G. S. *Biochemistry* **1999**, *38*, 4988. (b) Babu, C. R.; Aruchandran, A.; Hille, R.; Gross, E. L.; Bullerjahn, G. S. *Biochem. Biophys. Res. Commun*. **1997**, *235*, 631.
(28) Hervas, M.; Myshkin, E.; Vintoneko, N.; De La Rosa, M. A.; Bullerjahn, G. S.; Navarro, J. A. *J. Biol. Chem*. **2003**, *278*, 8179.
(29) Job, P. *Ann. Chim*. **1928**, *9*, 113.

(30) (a) Lipskier, J. F.; Tran-Thi, T. H. *Inorg. Chem.* **1993**, *32*, 722. (b) Balbinot, D.; Atalick, S.; Guldi, D. M.; Hatzimarinaki, M.; Hirsch, A.; Jux, N. *J. Phys. Chem. B* **2003**, *107*, 13273.

(31) Tyson, D. S.; Castellano, F. N. *J. Phys. Chem. A.* **1999**, *103*, 10955.

(32) (a) Foster, R. *Organic Charge-Transfer Complexes;* Academic Press: London and New York, 1969. (b) Rose, N. J.; Drago, R. S. *J. Am. Chem. Soc.* **1959,** *81*, 6138.

(33) (a) Cristensen, H. E.; Ulstrup, J.; Sykes, A. G. *Biochim. Biophys. Acta* **1990**, *1039*, 94−102. (b) Sykes, A. G. *Chem. Soc. Rev.* **1985**, *14*, 283.

(34) (a) Modi, S.; Nordling, M.; Lundberg, L. G.; Hansson, O.; Bendall, D. S. *Biochim. Biophys. Acta* **1992**, *1102*, 85. (b) Kannt, A.; Young, S.; Bendall, D. S. *Biochim. Biophys. Acta* **1996**, *1277*, 115.

(35) (a)Young, S.; Sigfridsson, K.; Olesen, K.; Hansson, O. *Biochim. Biophys. Acta* **1997**, *1322*, 106. (b) Sigfridsson, K. *Photosynth. Res.* **1998**, *57*, 1−28.

(36) (a) Martinez, S. E.; Huang, D.; Szczepaniak, A.; Cramer, W. A.; Smith, J. L. *Structure* **1994**, *2*, 95. (b) Moore, G. R.; Pettigrew, G. W. *Cytochromes C: Evolutionary, Structural and Physiological Aspects;* Springer-Verlag: Berlin, Germany, 1990.

(37) (a) Sigfridsson, K.; Hansson, O.; Karlsson, B. G.; Baltzer, L.; Nordling, M.; Lundberg, L. G. *Biochim. Biophys. Acta* **1995**, *1228*, 28.

(38) (a) Beaven, G. H.; Holiday, E. R. *Adv. Protein Chem.* **1952**, *7*, 319. (b) Wetlaufer, D. B. *Adv. Chem.* **1962**, *17*, 303.

(39) Kalyanasundaram, K. *Photochemistry of Polypyridine and Porphyrin Complexes;* Academic Press: New York, 1992.

(40) Auodia, M.; Guliaev, A. B.; Leontis, N. B.; Rodgers. M. A. J. *Biophys. Chem.* **2000**, *83*, 121.

(41) Ort, D. R.; Yocum, C. F. *Oxygenic Photosynthesis: The Light Reactions;* Kluwer Academic Publishers: Norwell, MA, 1996.

(42) (a) Birks, J. B. *Photophysics of Aromatic Molecules;* Wiley−Interscience: London, 1970. (b) Cotton, F. A.; Wilkinson, G. *Advanced Inorganic Chemistry;* Wiley−Interscience: London, 1966.

(43) Cowan, J. A. *Inorganic Biochemistry: An Introduction;* VCH Publishers: New York, 1993.

(44) (a) Chasteen, N. D. *Adv. Inorg. Chem.* **1983**, *5*, 201−233. (b) Warner, R. C.; Weber, I. *J. Am. Chem. Soc.* **1953**, *75*, 5094.

(45) (a) Gouterman, M. In *The Porphyrins*; Academic Press: New York, 1978; Vol. 3. (b) Gouterman, M. *J. Chem. Phys.* **1959**, *30*, 1139. (c) Kobayashi, H.; Sekino, H. *J. Chem. Phys.* **1987**, *86*, 5045.

(46) (a) Kasha, M. *Radiat. Res.* **1963**, *20*, 55. (b) Gouterman, M.; Holten, D.; Lieberman, E. *Chem. Phys.* **1977**, *25*, 139.

(47) Kasha, M.; Ashraf El-Bayomi, M.; Rhodes, W. *J. Chem. Phys.* **1961**, *58*, 916.

(48) Pelliccioli, A. P.; Henbest, K,; Kwag, G.; Carvagno, T. R.; Kenney, M. E.; Rodgers, M. A. J. *J. Phys. Chem. A* **2001**, *105*, 1757.

(49) Schopfer, L. M.; Massey, V. *Biochemistry* **1988**, *27*, 6599.

(50) Mitra, B.; Dewanti, A. R. *Biochemistry* **2003**, *42*, 12893.

(51) Aladekomo, J. B.; Birks, J. B. *Proc. R. Soc. London, Ser. A* **1965**, *284*, 551.

(52) (a) Sigfridsson, K. *Photosynth. Res.* **1998**, *57*, 1. (b) Colman, P. M.; Freeman, H. C.; Guss, J. M.; Murata, M.; Norris, V. A.; Ramshaw, J. A. M.; Venkatappa, M. P. *Nature* **1978**, *272*, 319.

(53) Hirota, S.; Hayamizu, K.; Okuno, T.; Kishi, M.; Iwasaki, H.; Kondo, T.; Hibino, T.; Takabe, T.; Khzuma, T.; Yamauchi, O. *Biochemistry* **2000**, *39*, 6357.

(54) Pearson, R. G. *J. Chem. Ed.* **1968**, *45*, 581.

(55) (a) Zhou. J. S.; Kostic, N. M. *J. Am. Chem. Soc.* **1992**, *114*, 3562. (b) Bagby, S.; Driscoll, P. C.; Goodall, K. G.; Redfield, C.; Hill, H. A. O. *Eur. J. Biochem.* **1990**, *188*, 413. (c) Roberts, V. A.; Freeman, H. C.; Olson, A. J.; Tainer, J. A.; Getzoff, E. D. *J. Biol. Chem.* **1991**, *266*, 13431.

(56) Mauk, M. R.; Reid, L. S.; Mauk, A. G. *Biochemistry* **1982**, *21*, 1843.

(57) Kalyanasundaram, K.; Neumann-Spallart, M. *J. Phys. Chem.* **1982**, *86*, 5163.

(58) Logunov, S. L.; Rodgers, M. A. J. *J. Photochem. Photobiol., A* **1997**, *105*, 55.

(59) (a) Harriman, A.; Porter, G.; Wilowska, A. *J. Chem. Soc., Faraday Trans. 2* **1984**, *90*, 191. (b) Tran-Thi, T. H.; Lipskier, J. F.; Houde, D.; Pepin, C.; Keszei, E.; Jay-Gerin, J. P. *J. Chem. Soc., Faraday Trans.* **1992**, *88*, 2129. (c) Logunov, S. L.; Rodgers, M. A. J. *J. Phys. Chem.* **1992**, *96*, 8697.

(60) Demas, J. N.; Addington, J. W.; Peterson, S. H.; Harris, E. W. *J. Phys. Chem.* **1977**, *81*, 1039.

(61) Harriman, A. *J. Phys. Chem.* **1987**, *91*, 6102.

(62) (a) Marcus, R. A.; Sutin, N. *Biochim. Biophys. Acta* **1985**, *811*, 265. (b) McLendon, G.; Miller, J. R.; *J. Am. Chem. Soc.* **1985**, *107*, 7811. (b) McLendon, G.; Miller, J. R.; *J. Am. Chem. Soc.* **1988**, *110*, 3345. (c) Meade. T. J.; Gray, H. B.; Winkler, J. R. *J. Am. Chem. Soc.* **1989**, *111*, 4353. (d) Aoudia, M.; Guliaev, A.; Leontis, N. B.; Rodgers, M. A. J. *Biophys. Chem.* **2000**, *83*, 121. (e) Gray, H. B.; Malmstrom, B. G.; Williams, R. J. P. *J. Biol. Inorg. Chem.* **2000**, *5*, 551.